Neuropharmacology xxx (xxxx) xxx

Contents lists available at ScienceDirect

Neuropharmacology

journal homepage: www.elsevier.com/locate/neuropharm

Invited review

Comparative mapping of selected structural determinants on the extracellular domains of cholinesterase-like cell-adhesion molecules

Davide Comoletti [a,b,c,*], Laura Trobiani [a], Arnaud Chatonnet [d], Yves Bourne [e], Pascale Marchot [e,**]

[a] School of Biological Sciences, Victoria University of Wellington, Wellington, 6012, New Zealand
[b] Child Health Institute of New Jersey, New Brunswick, NJ 08901, USA
[c] Department of Neuroscience and Cell Biology Robert Wood Johnson Medical School, Rutgers University, New Brunswick, NJ 08901, USA
[d] Lab 'Dynamique Musculaire et Métabolisme', Institut National de Recherche pour l'Agriculture, l'Alimentation et l'Environnement (INRAE) / Université Montpellier, Montpellier, France
[e] Lab 'Architecture et Fonction des Macromolécules Biologiques (AFMB)', Centre National de la Recherche Scientifique (CNRS)/Aix-Marseille Univ, Faculté des Sciences - Campus Luminy, Marseille, France

ARTICLE INFO

Keywords:
Cell-adhesion molecule
Cholinesterase-like domain
Functional partnership
Homology model
Structural superfamily
Surface determinants

ABSTRACT

Cell adhesion generally involves formation of homophilic or heterophilic protein complexes between two cells to form transcellular junctions. Neural cell-adhesion members of the α/β-hydrolase fold superfamily of proteins use their extracellular or soluble cholinesterase-like domain to bind cognate partners across cell membranes, as illustrated by the neuroligins. These cell-adhesion molecules currently comprise the synaptic organizers neuroligins found in all animal phyla, along with three proteins found only in invertebrates: the guidance molecule neurotactin, the glia-specific gliotactin, and the basement membrane protein glutactin. Although these proteins share a cholinesterase-like fold, they lack one or more residues composing the catalytic triad responsible for the enzymatic activity of the cholinesterases. Conversely, they are found in various subcellular localisations and display specific disulfide bonding and N-glycosylation patterns, along with individual surface determinants possibly associated with recognition and binding of protein partners. Formation of non-covalent dimers typical of the cholinesterases is documented for mammalian neuroligins, yet whether invertebrate neuroligins and their neurotactin, gliotactin and glutactin relatives also form dimers in physiological conditions is unknown. Here we provide a brief overview of the localization, function, evolution, and conserved *versus* individual structural determinants of these cholinesterase-like cell-adhesion proteins.

This article is part of the special issue entitled 'Acetylcholinesterase Inhibitors: From Bench to Bedside to Battlefield'.

1. Introduction

Neuronal cell-adhesion generally involves formation of homo- or heterophilic protein complexes to form synaptic or non-synaptic cell contacts/junctions (Apóstolo and de Wit, 2019), and several superfamilies of cell-adhesion molecules have been characterized (de Wit and Ghosh, 2016). A particular subset of cell-adhesion proteins shares a characteristic cholinesterase (ChE) -like extracellular domain, despite significant sequence differences and absence of an enzymatic activity (Sussman et al., 1991; Krejci et al., 1991; Ollis et al., 1992) (Fig. 1, Table 1). This domain, which defines the large α/β-hydrolase fold superfamily of proteins, is characterized by a central β-sheet core made of about ten parallel and usually one antiparallel β-strands, themselves connected by a related number of α-helices (Hotelier et al., 2004). In the enzymatically active members of the family, precise and conserved positioning of three catalytic residues is mandatory to form a functional nucleophile (Ser)/acid (His)/base (Asp or Glu) triad. A shell of secondary structural elements, mostly comprising α-helices and loops of

Abbreviations: AChE, acetylcholinesterase; ChE, cholinesterase; (Hu, human; Mo, mouse; Dm, *Drosophila melanogaster*); GLIO, gliotactin; GLUT, glutactin; NLGN, neuroligin; NRT, neurotactin; NRXN, neurexin.

* Corresponding author. School of Biological Sciences, Victoria University of Wellington, Wellington 6012, New Zealand.
** Corresponding author.
E-mail addresses: davide.comoletti@vuw.ac.nz (D. Comoletti), pascale.marchot@univ-amu.fr (P. Marchot).

https://doi.org/10.1016/j.neuropharm.2020.108381
Received 1 July 2020; Received in revised form 10 September 2020; Accepted 29 October 2020
Available online 6 November 2020

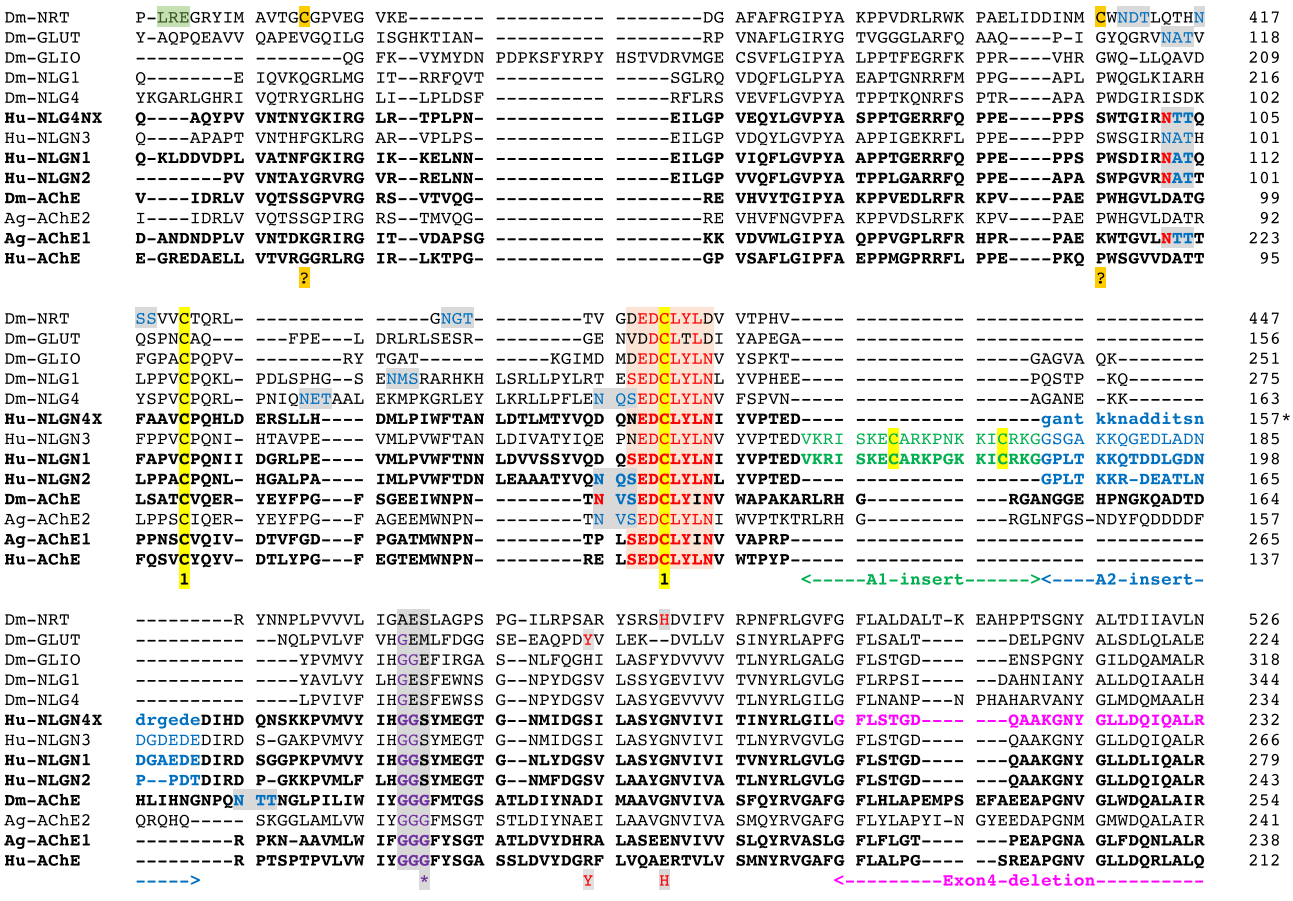

Fig. 1. - Sequence alignment of selected ChE and ChE-like extracellular domains - Sequences in bold denote proteins for which a crystal structure is available. Residue numbering right to each sequence is that of UniProt, which includes the signal peptide. *(For RCSB-PDB accession codes and UniProt entries, see below.)* The N- and C-terminal extremities of the proteins, which display low sequence conservation, are not displayed. Only for Dm-NRT are two additional N-term residues included because they belong to a LRE motif, while the true C-terminal end is displayed as denoted by a double slash (//). Letter/color codes within the alignment: C letters on yellow and orange background, Cys residues involved (all proteins) and likely to be involved (NRT) in disulfide bonds, respectively; green LRE letters (or two of them only) on green background, putative motifs for partner recognition; blue NXS/T letters on grey background, consensus triplets for N-glycosylation (NB - a red N letter denotes experimentally demonstrated occupancy); red SEDCLYLN letters on orange background, conserved octapeptide signature in the ChE and ChE-like subfamilies; purple GGG letters on grey background, conserved triplet in ChE proteins – the star below the alignment points to the Gly to Ser substitution found in the NLGNs and the insecticide-resistant Ag-AChE mutant; red H letter on grey background, C-terminal boundary of the NRT sequence (His347-His482) required for amalgam binding and cell adhesion; red Y letters on grey background, predicted sulfo-Tyr residue; GXSXGX sequence on grey background, conserved hexapeptide signature of the α/β hydrolase fold superfamily; red S/E/H letters, catalytic triad residues in AChEs. Letter/color codes below the alignment: question marks on orange background, Cys residues proposed to form the non-conserved, N-terminal disulfide bond in NRT; 1/2/3 ab letters on yellow background, Cys residues forming the conserved first and second and alternative third disulfide bridges; green/blue "A1/A2" stretches, splice inserts A1/A2 in human NLGNs 1–4 (NB - NLGN4X insert A2, found in low occurrence isoform 2, is displayed in lowercase letters and not included in the numbering (see * right to the sequence line); pink residues and 'exon4-deletion' note, splice insert in NLGN4X; orange "B" stretch, splice insert B in rodent NLGN1 (not found in human NLGN1); "aromatic" stretch, Trp/Tyr/Phe-rich insert also found in many insect proteins; "Gly-rich" stretch, Gly-rich insert also found in several *Drosophila* proteins (see below); "H1/H2-helix" stretches, approx. coverage of helices α3(7,8) and α10 involved in dimer formation for the ChEs and NLGNs (NB – the red R letter in Hu-NLGN3 helix H1 denotes the position of the R451C substitution).

RCSB-PDB entries: Hu-NLGN4X, 3BE8; Hu-NLGN1, 3BIX for the rat homologue; Hu-NLGN2, 3BL8 for the mouse homologue; Dm-AChE, 1QO9; Ag-AChE1, 5X61; Hu-AChE, 1B41.

UniProt entries: Dm-NRT, P23654; Dm-GLU, P33438; Dm-GLIO, Q9NK80; Dm-NLGN1, Q9VIC7; Dm-NLGN4, Q9VDP5; Hu-NLGN4X, Q8N0W4 (variant, Q8N0W4-2); Hu-NLGN3, Q9NZ94; Hu-NLGN1, Q8N2Q7; Hu-NLGN2, Q8NFZ4; Dm-AChE, P07140; Ag-AChE2, Q7QFG0; Ag-AChE1, Q869C3; Hu-AChE, P22303.

Drosophila proteins with a Gly-rich stretch: GH07829p (gene Nlg4, UniProt entry B6IDZ4), GM23100 (Dsec\GM23100, B4IIE9), GD19341 (Dsim\GD19341, B4QS57), uncharacterized protein (Dana\GF17640, A0A0P8XXC1), GL12091 (Dper\GL12091, B4GL70), NLGN1 (*DGUA_6G016471*, A0A3B0KJP9).

variable sizes, wraps around this central core and defines less conserved surface determinants for, e.g., substrate attraction and guidance to the active center, binding of co-factors and partners, protein resistance to external factors, or cellular localization. A third level of specialization is sometimes achieved through insertion of additional, structurally and functionally unrelated domains which further extend the protein functionality (e.g., the flap in lipases), or add another function, or dictate a mode of attachment to membranes (Carr and Ollis, 2009; Marchot and Chatonnet, 2012).

The currently identified ChE-like cell-adhesion molecules comprise four members: the synaptic organizers neuroligins (NLGN), which are found in all animal phyla and for which several crystal structures are available, and the guidance molecule neurotactin[1] (NRT; Hortsh et al., 1990), the glia-specific protein gliotactin (GLIO; Auld et al., 1995),

[1] Not to be confused with the chemokine 'fraktalkine', aka chemokine (C-X3-C motif) ligand 1, occasionally named 'neurotactin' as well (see Hortsch, 1997).

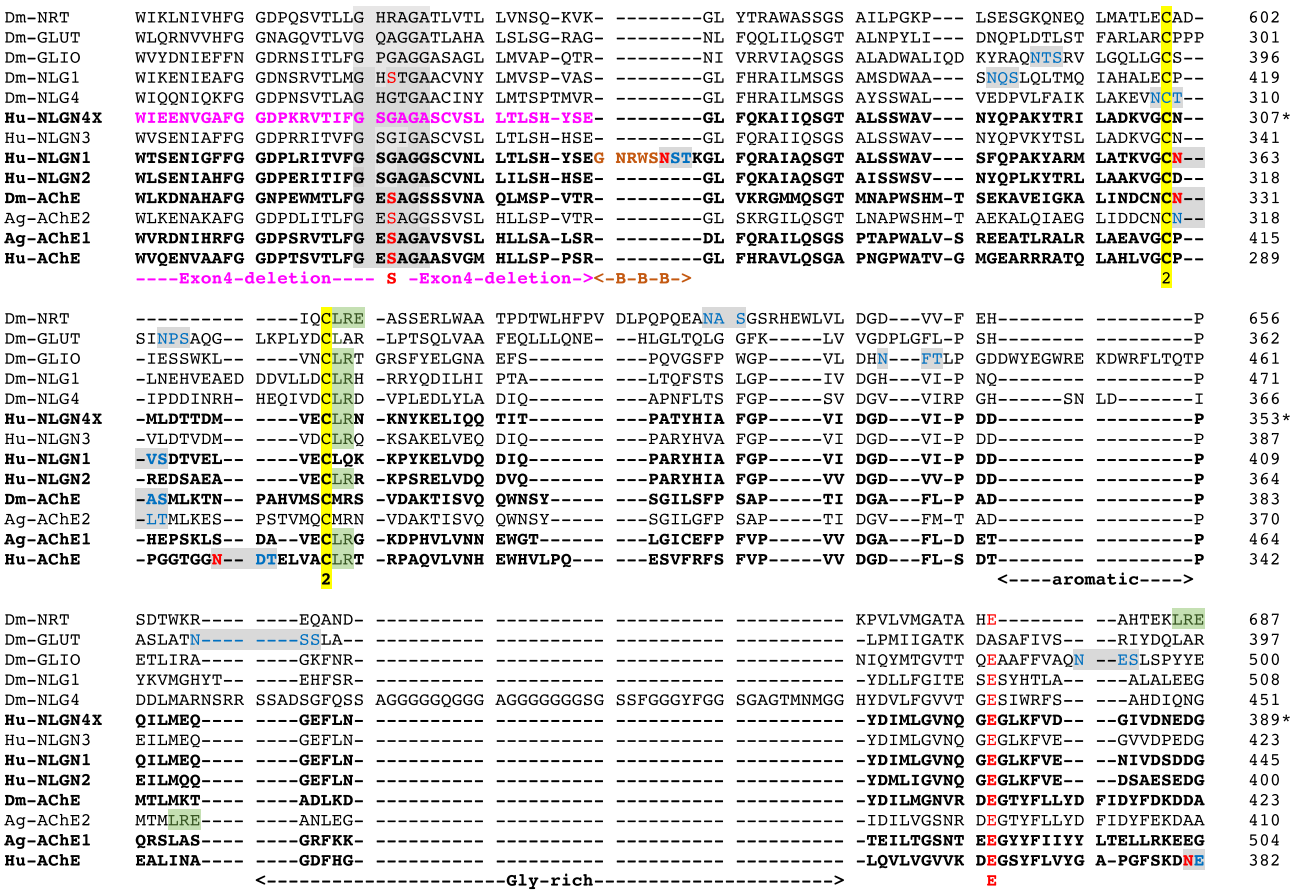

Fig. 1. (*continued*).

and the basement membrane protein glutactin (GLUT; Olson et al., 1990), which are found only in invertebrates. The NLGNs, GLIO and NRT are single-pass transmembrane proteins, albeit the first two are of type-I (intracellular C-terminus) while the latter is of type-II (extracellular C-terminus), whereas GLUT is a secreted protein found associated to the basement membrane of cells (for references, see below). These cell-adhesion proteins generally lack the Ser residue, and occasionally one of the other two residues, of the catalytic triad responsible for the enzymatic activity of the ChEs. Conversely, they display surface molecular determinants associated with specific partner recognition and binding.

Several reviews comparing the ChEs and their cell-adhesion relatives at the structural and functional levels have been published before (Grifman et al., 1998; Grisaru et al., 1999; Scholl and Scheiffele, 2003; Gilbert and Auld, 2005) and after crystal structures of NLGNs provided in depth views of the structural peculiarities of a ChEL-like adhesion molecule (De Jaco et al., 2012; Bourne & Marchot, 2014, 2017). Here we describe the known subcellular localizations and functions of the ChE-like cell-adhesion molecules NLGNs, NRT, GLIO and GLUT. We compare homology models of the NRT, GLIO and GLUT with experimental (crystal) structures of selected acetylcholinesterase (AChE) and NLGN proteins, in pointing to structural determinants such as their modified active center, disulfide bonding patterns, capacity for dimer formation, N-glycosylation and LRE motif patterns, and electrostatic surface potentials. We also assess their evolutionary relationships and review their known protein partners.

2. Subcellular localizations and functions

2.1. The neuroligins (UniProt ID for human proteins: NLGN1 Q8N2Q7; NLGN2 Q8NFZ4; NLGN3 Q9NZ94; NLGN4X Q8N0W4; NLGN4Y Q8NFZ3)

Rat NLGN1 (Uniprot ID: Q62765), a type-I cell membrane protein of 843 amino acid residues whose extracellular ChE-like domain comprises residues 45–639 (Fig. 1; Table 1), was initially identified by affinity chromatography as a post-synaptic neuronal receptor for the presynaptic neurexin-β1 (NRXN-β1) (Ichtchenko et al., 1995). Subsequently, three other *NLGN* genes were identified in rodents (Ichtchenko et al., 1996) and five in humans (Bolliger et al., 2001). In humans, the *NLGN1* and *NLGN2* genes are located on chromosomes 3 and 17, respectively, while both the *NLGN3* and *NLGN4X* genes are on the X chromosome. The fifth, *NLGN4Y* 'gene', a *NLGN4X* allele located on the Y chromosome, encodes a NLGN4Y or NLGN5 protein that is 97% similar to NLGN4X (Bolliger et al., 2001). In mouse there is a more divergent *NLGN4-like* gene/allele, located on the pseudoautosomal region of the X chromosome (Bolliger et al., 2001, 2008; Maxeiner et al., 2020). NLGN1 localizes at excitatory glutamatergic synapses (Song et al., 1999; Graf et al., 2004), NLGN2 selectively at inhibitory GABAergic and excitatory cholinergic synapses (Varoqueaux et al., 2004; Dong et al., 2007; Takács et al., 2013), NLGN3 at both excitatory glutamatergic and inhibitory GABAergic synapses (Budreck and Scheiffele, 2007; Földy et al., 2013), and NLGN4X preferentially at glycinergic inhibitory synapses (Hoon et al., 2011), where they

```
Dm-NRT      LHANWTREEV RAYLEN---- -------SQI GALGLTDE-V IEKYNASS-- YASLVSIISD IRSVCPLLTN A--------- ----------  744
Dm-GLUT     LQSRN----V SDYIDVVLRH TAPPSEHR-- ---LWKQW-A LREIFTPI-- QEQTASL--- -QTVAPGLLE LSNYIL---- ----------  457
Dm-GLIO     LDGRFFDQKI REHVFR-YNY TLNPNGVYEA IKYIYTFW-P DPNNNTII-- RDQYINMLSD LYYRAPVDQM VKLML----- ----------  571
Dm-NLG1     LRENERDNLL RFYMQSRFDI RP--DLALAA TLKKYQDMYN NPIKATNLEH RDVVLDILSD ARVVGPLLQT GMFHA----- ----------  581
Dm-NLG4     FEGERRDKII RTYVRNAYNY HL--NEIFYT IVNEYTDWDR TSQHPINT-- RDTAVAALSD AQFVAPIVRA GDILAANSPP PVSSSSTAGS  537
Hu-NLGN4X   VTPNDFDFSV SNFVDNLYGY PEGKDTLRET IKFMYTDW-A DKENPETR-- RKTLVALFTD HQWVAPAVAT ADLHA----- ----------  461*
Hu-NLGN3    VSGTDFDYSV SNFVDNLYGY PEGKDTLRET IKFMYTDW-A DRDNPETR-- RKTLVALFTD HQWVEPSVVT ADLHA----- ----------  495
Hu-NLGN1    ISASDFDFAV SNFVDNLYGY PEGKDVLRET IKFMYTDW-A DRHNPETR-- RKTLLALFTD HQWVAPAVAT ADLHS----- ----------  517
Hu-NLGN2    VSASAFDFTV SNFVDNLYGY PEGKDVLRET IKFMYTDW-A DRDNGEMR-- RKTLLALFTD HQWVAPAVAT AKLHA----- ----------  472
Dm-AChE     TALPRDKYL- -EIMNNIFGK AT--QAEREA IIFQYTSW-E -GNPGYQN-- QQQIGRAVGD HFFTCPTNEY AQALA----- ----------  490
Ag-AChE2    TSLPRDKFL- -EIMNTIFNK AS--EPEREA IIFQYTGW-E SGNDGYQN-- QHQVGRAVGD HFFICPTNEF ALGLT----- ----------  478
Ag-AChE1    VTVTREEFL- -QAVRELNPY VN--GAARQA IVFEYTDW-T EPDNPNSN-- RDALDKMVGD YHFTCNVNEF AQRYA----- ----------  572
Hu-AChE     SLISRAEFL- -AGVRVGVPQ VS--DLAAEA VVLHYTDW-L HPEDPARL-- REALSDVVGD HNVVCPVAQL AGRLA----- ----------  450
                               <--H1-helix-->                                  3a

Dm-NRT      ---------- ----RQQPSV PFYVVT---- -------QGE GPDQLATVDA D-VQAILG-- ---------- ----RYEPHT VEQRRFVSAM  792
Dm-GLUT     --YRAPVINS ISQSYRSVPA YLYTFDYRGE HHRFGHLSNP LPFGVDASLS DDSVYLFPYP PEAS------ -------RLN PLDRSLSRAL  532
Dm-GLIO     ---------- ----EQKVPV YMYVLNTTVE -------ALN LPQWRKYPHD IERYFLTGAP FMDT-EFFPK KEHLQRNMWT DNDRNMSHFF  639
Dm-NLG1     ---------- ----DVNRRN YMYVFGHNSA -------TGP FAHLPHSIMG EELAFIFGAP LAAAGPFPSG N-------YT VQEKLLSEAV  643
Dm-NLG4     PGANAAASTS AGSTQPSGRC YFYVFDYQTK -------DGD YPQRMGTVHG EDLPYIFGAP LVDGFSHFPQ N-------YT KSETALSEAV  613
Hu-NLGN4X   ---------- ----QYGSPT YFYAFYHHCQ -------SEM KPSWADSAHG DEVPYVFGIP MIGPTELFSC N-------FS KNDVMLSAVV  523*
Hu-NLGN3    ---------- ----RYGSPT YFYAFYHHCQ -------SLM KPAWSDAAHG DEVPYVFGVP MVGPTDLFPC N-------FS KNDVMLSAVV  557
Hu-NLGN1    ---------- ----NFGSPT YFYAFYHHCQ -------TDQ VPAWADAAHG DEVPYVLGIP MIGPTELFPC N-------FS KNDVMLSAVV  579
Hu-NLGN2    ---------- ----DYQSPV YFYTFYHHCQ -------AEG RPEWADAAHG DELPYVFGVP MVGATDLFPC N-------FS KNDVMLSAVV  534
Dm-AChE     ---------- ----ERGASV HYYYFTHRTS -------TSL WGEWMGVLHG DEIEYFFGQP LNNS-----L Q-------YR PVERELGKRM  547
Ag-AChE2    ---------- ----ERGASV HYYYFTHRTS -------TSL WGEWMGVLHG DEVEYIFGQP MNAS-----L Q-------YR QRERDLSRRM  535
Ag-AChE1    ---------- ----EEGNNV YMYLYTHRSK -------GNP WPRWTG-MHG DEINYVFGEP LNPT-----L G-------YT EDEKDFSRKI  629
Hu-AChE     ---------- ----AQGARV YAYVFEHRAS -------TLS WPLWMGVPHG YEIEFIFGIP LDPS-----R N-------YT AEEKIFAQRL  507
                                    3b                    H                    3b

Dm-NRT      QQLFYYYVSH GTVQSFV--- ---------- ---------- --QNRRVINV GQDAQPEEDY LP-------- ---CNYWISK DIVPRYARVD//  846
Dm-GLUT     VTMWVNFATT GVPNPS---- ---------- ---SGVWPQA TSEYGPFLRF TNNQQSPLEL DP-HFGEGI- ---------- -YLPNYRVI-  591
Dm-GLIO     MQTYTNFARY GNPT------ --------PQ QVLGMHFQRA YQGEIRYLNI NT------TY NS-SILLNYR QTECAFW-T- QYLP------  700
Dm-NLG1     MAYWTNFVKT GNPKAPWKGI FINSHALEWD RY-DLDWPEF NRRAQAYLNI --------GI PP TVGYKYR QIYMNFWNKE LPDELNQIA-  722
Dm-NLG4     MIFWTNFART GNPNEHHRQD SSLPVSKERN RFRSITWENY DPLHQKYLEI --------GM KP-RIKNHFR AHQLSIWL-- RLIPELHRA-  691
Hu-NLGN4X   MTYWTNFAKT GDPNQPVPQD TKF-IHTKPN RFEEVAWSKY NPKDQLYLHI --------GL KP-RVRDHYR ATKVAFWL-- ELVPHLHNL-  600*
Hu-NLGN3    MTYWTNFAKT GDPNKPVPQD TKF-IHTKAN RFEEVAWSKY NPRDQLYLHI --------GL KP-RVRDHYR ATKVAFWK-- HLVPHLYNL-  634
Hu-NLGN1    MTYWTNFAKT GDPNQPVPQD TKF-IHTKPN RFEEVAWTRY SQKDQLYLHI --------GL KP-RVKEHYR ANKVNLWL-- ELVPHLHNL-  656
Hu-NLGN2    MTYWTNFAKT GDPNQPVPQD TKF-IHTKPN RFEEVVWSKF NSKEKQYLHI --------GL KP-RVRDNYR ANKVAFWL-- ELVPHLHNL-  611
Dm-AChE     LSAVIEFAKT GNPAQ----- ---------- --DGEEWPNF SKEDPVYYIF ST------DD KIEKLARGPL AARCSFWN-- DYLPKVRS--  610
Ag-AChE2    VLSVSEFART GNPAL----- ---------- --EGEHWPLY TRENPIYFIF NAEGED--DL RGEKYGRGPM ATSCAFWN-- DFLPRLRAW-  603
Ag-AChE1    MRYWSNFAKT GNPNP----- -------NTA SSEFPEWPKH TAHGRHYLEL --------GL NTSFVGRGPR LRQCAFWK-- KYLPQLVA--  695
Hu-AChE     MRYWANFART GDPN------ -------EPR DPKAPQWPPY TAGAQQYVSL --------DL RPLEVRRGLR AQACAFWN-- RFLPKLLSAT  574
                                                  Y                        <--- 3a --H2-helix-----
```

Fig. 1. (*continued*).

selectively control synaptic connectivity. In the central nervous system, NLGN4X is barely present (Bolliger et al., 2001) while NLGN3 is also expressed by glial cells, where it functions in a non-cell-autonomous manner, consistent with a signaling role (Sakers and Eroglu, 2019). Outside the central nervous system, NLGN1 has been found in the vascular system (Bottos et al., 2009), NLGN2 in uterus (Kang et al., 2004), NLGN3 in muscle and pancreas (Philibert et al., 2000), and NLGN4X in heart, liver, skeletal muscle and pancreas (Bolliger et al., 2001).

Alternative mRNA splicing events result in the presence or absence of splice inserts in the extracellular domain of NLGNs 1–4 (two consecutive inserts A1/A2 in NLGNs 1–4 and one N-glycosylated insert B in rodent NLGN1 (Fig. 1, green A1/blue A2 and orange B stretches), which form extra loops at the subunit surface and give rise to several isoforms with distinctive partnership properties (Boucard et al., 2005; Chih et al., 2006; Talebizadeh et al., 2006; Koehnke et al., 2010). NLGN insert A2 is at the same position as a splicing or individual insert found in insect AChEs, while additional inserts, of which a long Gly-rich stretch most likely to be structurally disordered, are found at other positions in *Drosophila* NLGN4 (but not NLGN1) and several other *Drosophila* proteins (Fig. 1).

The essential neurodevelopmental role of the NLGNs was highlighted by the identification of genetic aberrations associated with a diagnosis of autism spectrum disorders and intellectual disability (Südhof, 2017; Cao and Tabuchi, 2017). Since the early 2000's, several single residue substitutions in the ChE-like domain of the NLGNs have been found to be associated with autism. The first missense variant, Arg451Cys, was identified in two affected brothers (Jamain et al., 2003). The resulting substitution, localized in the extracellular domain of NLGN3 (Fig. 1), was shown to alter trafficking of the mutant protein through the intracellular secretory pathway (Comoletti et al., 2004; Chih et al., 2004; De Jaco et al., 2006). Other rare variants were also found for the other NLGNs, of which most were linked to autism and related neurodevelopmental disorders (Laumonnier et al., 2004; Yan et al., 2005; Talebizadeh et al., 2006; Lawson-Yuen et al., 2008; Daoud et al., 2009; Zhang et al., 2009; Pampanos et al., 2009; Sun et al., 2011; Xu et al., 2014; Landini et al., 2016; Nakanishi et al., 2017; Quartier et al., 2019; Shillington et al., 2020; and others).

Table 1
Calculated sequence identity (in parentheses: similarity) of the extracellular domains of acetylcholinesterase and cholinesterase-like proteins (%).

	Hu-NLGN4X	Dm-AChE	Mo-AChE	Dm-NRT	Dm-GLIO	Dm-GLUT
Hu-NLGN4X	100					
Dm-AChE	25.3 (50.7)	100				
Mo-AChE	31.5 (58.1)	34.0(60.4)	100			
Dm-NRT	20.1 (44.0)	21.0 (46.6)	23.8 (47.5)	100		
Dm-GLIO	27.3 (51.2)	22.1 (51.9)	27.9 (54.2)	24.4 (48.9)	100	
Dm-GLUT	22.0 (46.1)	20.5 (47.6)	23.5 (50.8)	22.8 (45.8)	21.2 (51.7)	100

2.2. Neurotactin (for Dm-NRT: CG9704; UniProt ID: P23654; FlyBase ID FBgn0004108)

NRT, a 846-residue transmembrane protein with a type-II topology and whose extracellular ChE-like domain comprises residues 347–846 (Fig. 1; Table 1), is found only in insects (de la Escalera et al., 1990). In the *Drosophila* nervous system it is expressed during development but not in adulthood. Functionally, NRT appear to be a heterophilic cell adhesion molecule that accumulates on the cell surface where it induces axonal outgrowth, guidance, and fasciculation (Barthalay et al., 1990; Speicher et al., 1998). The only known ligand for NRT is amalgam, a secreted protein member of the Ig superfamily (Frémion et al., 2000). Strikingly, only the first third of the extracellular domain of NRT, whose sequence homology with the ChEs or ChE-like proteins is higher than those of the second and third thirds (Fig. 1), was found to be necessary for both amalgam binding and cell adhesion (Frémion et al., 2000). This suggests that C-terminally truncated NRT still folds and undergoes intracellular trafficking and presentation at the cell membrane, to display an extracellular 'lobe' comprising half of the central β-sheet and surrounding surface loops. In contrast to the NLGNs, whose ChE-like domain is separated from the transmembrane domain by a stalk domain (Ichtchenko et al., 1995) permitting flexible positioning in the synaptic cleft, in NRT the ChE-like domain starts right after the transmembrane domain.

2.3. Gliotactin (for Dm-GLIO: CG3903; UniProt ID Q9NK80; FlyBase ID FBgn0001987)

GLIO, a single pass transmembrane protein of 956 residues and whose extracellular ChE-like domain comprises residues 136–695 (Fig. 1), is found in both nematodes and arthropods (Auld et al., 1995). In *Drosophila* it is expressed in a wide range of epithelial-like tissues including peripheral glia, epidermis, hindgut, etc. At the cellular level, GLIO is localized to septate junctions, which are structurally equivalent to vertebrate tight junctions. Specifically, GLIO is uniquely localized to the tricellular junction, a specialized structure formed by the convergence of septate junctions in three neighboring cells (Schulte et al., 2003). The highest expression of GLIO during embryonic development is in the peripheral glia from stage 13, with an expression peak at stage 17 during the formation of the blood-nerve permeability barrier (Auld et al., 1995). In addition to permeability defects in the fly salivary glands, gut, and trachea, lack of GLIO in the embryo causes nearly complete paralysis due to the high potassium leak into the motor axons (Auld et al., 1995; Venema et al., 2004). GLIO appears to function as a heterophilic cell-adhesion molecule, although its ligand is unknown. The ChE-like domain of GLIO is separated from the transmembrane span by a 10-residue peptide, i.e., a length intermediate between those for the NLGNs and NRT.

2.4. Glutactin (for Dm-GLUT: CG9280; UniProt ID P33438; FlyBase ID FBgn0001114)

GLUT, a secreted protein of 1026 residues whose extracellular ChE-like domain comprises residues 18–602 (Fig. 1), is only found in diptera (Olson et al., 1990). The C-terminal domain that follows is rich in Gln and Glu residues (44% of its composition, hence the name of the protein) and it is organized as semi-repetitive patterns of five residues suggesting the presence of several hydrophilic α-helices. In *Drosophila*, GLUT was identified as a sulfated, N- and O-glycosylated, strongly acidic calcium-binding protein important for structuring the segmented divisions of the fly. GLUT is found adjacent to sheets of epithelial cells in the basement membrane, lining segmentally spaced channels between segmental nerves in the abdominal segments. It is also found lining channels at the exact medial position between the central nervous system posterior commissures of one segment and the anterior commissures of the next segment. And it is found at the boundaries of segmentally arranged muscle cells where it is secreted at embryonic basement membranes, as part of the extracellular matrix (Olson et al., 1990). Ectopic expression of GLUT inhibits synapse formation by motor neurons that normally innervate muscle M12 (Inaki et al., 2007). The secreted character of GLUT first suggested a hormone/semiochemical processing-like mode of action (Montella et al., 2012), yet its association with the basement membrane of the extracellular matrix of cells makes it appropriate for cell-adhesion.

2.5. Evolution relationships of the ChEs and ChE-like molecules

The evolutionary tree generated from the sequence alignment shows that vertebrate NLGNs 1–4 most likely result from a double whole genome duplication event that occurred in the ancestor of this lineage (Fig. 2). In the arthropods, NLGNs 1–4 and GLIO result from duplications that occurred from the same gene present in the last common ancestor of the primitive invertebrates (protostomes) and the chordates, echinoderms and hemichordates (deuterostomes) (Lenfant et al., 2014). They may have either conserved the initial function of their common NLGN ancestor or acquired glial and neuronal functions independently. This tree also reflects the limited sequence homology of the second and third thirds of the ChE-like domain of NRT with the other domains, and the correlation between glial NLGNs and GLIO (Fig. 1).

3. Common versus individual characteristics of the ChE-like cell-adhesion proteins

While the ChE enzymes contain a well-conserved catalytic triad that can hydrolyze substrates of various sizes and chemical structures, their ChE-like cell-adhesion relatives are catalytically inactive and display distinctive structural features likely to be related to their respective functions. Below we compare the protein sequences and either experimental (crystal) structures or homology models of the extracellular domains of selected representative members of the ChE and ChE-like subfamilies.

3.1. Absence of a functional active center

The most prominent hallmark of the ChE-like cell-adhesion proteins is the lack of the Ser residue and occasionally one of the other two (Glu or His) residues of the catalytic triad responsible for the enzymatic activity of the ChEs (Fig. 1). Exceptions include *Drosophila* NLGN1, whose analysis through sequence alignment suggests retention of the Ser and Asp residues but substitution of the His residue by a Met; and GLUT, where both the Ser and Glu residues appear to be replaced by an Ala, while presence/absence of the His is unclear due to lower sequence identity in these regions.

Strikingly, in human and insect NLGNs a Ser residue replaces the third of those three Gly residues that in the ChEs form a typical triplet contributing to the oxyanion hole (Fig. 1). The same Ser substitution is found in insect AChEs resistant to insecticides (Weill et al., 2003), where the Ser side chain, located midway the active center gorge, sterically hinders ligand access to the catalytic Ser (Cheung et al., 2018). In the NLGNs, compared to the ChEs, the catalytic triad is modified and the active center pocket is reduced to a vestigial cavity, yet this new Ser side chain contributes coordinating a bound phosphate (PO4) trapped at the center of the subunit (Fabrichny et al., 2007). This observation may support, at least in part, the proposed correlation between exposure to ambient pesticides during pregnancy and early childhood as an environmental risk factor for autism (Bakian and Van Derslice 2019), in addition to the predominant genetic factors.

3.2. A partially conserved disulfide-bonding pattern

Another distinctive feature of the ChE-like cell-adhesion molecules is the conservation of the first two of the three disulfide bonds found in the

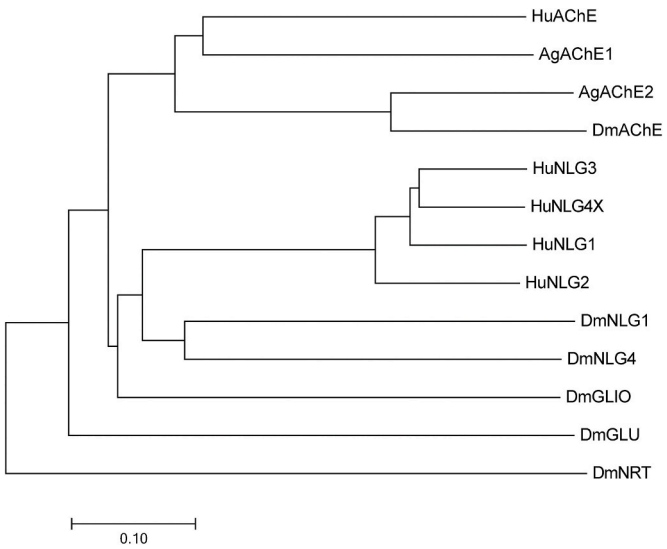

Fig. 2. - Evolutionary relationships of taxa - The evolutionary history was inferred using the Neighbor-Joining method (Saitou and Nei, 1987). The optimal tree with the sum of branch length = 3.37097384 is shown. The tree is drawn to scale, with branch lengths proportional to the evolutionary distances used to infer the phylogenetic tree. The evolutionary distances were computed using the p-distance method (Nei & Kumar, 2000) and are in the unit of the number of amino acid residue differences per site. The analysis involved 13 protein sequences (ChE-like domains only). All positions with less than 70% site coverage (e.g., individual or splice inserts) were not considered for the alignment. That is, fewer than 30% alignment gaps, missing data, and ambiguous bases were allowed at any position. There were a total of 503 positions in the final dataset. Evolutionary analyses were conducted in MEGA7 (Kumar et al., 2016).

ChEs (Fig. 1). The first disulfide bond ties a large loop, which in the ChEs is named the Ω loop for its shape, and which forms the upper part of the active center gorge, essential for the high catalytic activity of these enzymes (Sussman et al., 1991). This loop also contributes part of the binding surface for the snake toxin and peptidic AChE inhibitor, fasciculin[2] (Bourne et al., 1995; Harel et al., 1995). In the ChE-like adhesion members this loop is called Cys-loop because of its more variable shape (Fabrichny et al., 2007), and it was proposed to be important for heterologous partner recognition (Chatonnet et al., 2019). The second half-cystine in this first bond belongs to a conserved SEDCLYLN sequence, which is a signature motif of the ChE and ChE-like proteins and their carboxylesterase cousins. A consensus N-glycosylation sequence is often found just before or within the loop and shown to be occupied.

The second disulfide bond, which ties the base of a short loop protruding at the surface of the subunit, is the most conserved across the α/β-hydrolase fold superfamily of proteins (Fig. 1). The loop sequence is relatively variable, yet in the crystalline ChEs and NLGNGs this loop forms a typical helix-loop-helix motif. The loop often contains a consensus N-glycosylation sequence, found to be occupied in crystal structures.

The third disulfide bond, which in the ChEs stabilizes the C-terminal third of the subunit and insures proper positioning of the catalytic His residue, is both variable in its position and facultative in its presence (Fig. 1). This third bridge, along with the His residue, is present in the mammalian NLGNs, albeit at a distinct position that leads to a more flexible dimerization interface. In contrast it is absent, and occasionally the His as well, in insect NLGNs and in GLIO and GLUT, albeit one of the Cys is retained in GLIO. This suggests that the third bridge, important for the functional integrity of the ChE enzymes, is less important than the other two for the structural integrity of the ChE-like proteins. From an evolutionary perspective, this also suggests that vertebrate NLGNs conserved some enzymatic activity for a longer time than insect NLGNs.

[2] Not to be confused with the membrane-linked cell-adhesion molecule 'fasciclin', of an Ig-related fold.

The ChE-like domain of NRT contains two additional Cys residues (positions 367 and 408, Fig. 1) belonging to two distinct surface loops, yet found to lay proximal to each other in our homology model (data not shown). This observation suggests presence of a non-conserved, fourth disulfide bond contributing to structural stabilization of the N-terminal lobe of the NRT extracellular domain.

3.3. *Determinants for dimer formation*

Another hallmark of the ChE-like cell-adhesion molecules is the possible conservation of the two α-helices forming the four-helix bundle found at the dimer interface of all crystallized ChE species (Sussman et al., 1991; Bourne et al., 1995, 1999; Harel et al., 2000; Nicolet et al., 2003; Dvir et al., 2010; Han et al., 2018) and structurally studied NLGNs (Comoletti et al., 2003, 2006, 2007; Fabrichny et al., 2007; Araç et al., 2007; Koehnke et al., 2008) (Figs. 1, 3 and 4). The first of these two α-helices, labeled α3(7,8) in the mouse AChE and human NLGN4X structures, is ~10 residues long and internal to the protein sequence (H1-helix in Fig. 1), while the second helix, labeled α10, is ~15-residues long and located at the subunit C-terminus (H2-helix in Fig. 1). In the ChEs, helix α10 is where the second Cys in the third disulfide bond resides. Human NLGN4X was shown to form the same non-covalent dimer of subunits as mouse AChE, albeit with hydrophobic interactions accounting for a larger part of the large interface area buried between the two subunits, an observation suggesting that NLGN dimers are even more stable than AChE dimers (Fabrichny et al., 2007). In fact, the NLGNs were reported to be functional as homo- or heterodimers in physiological conditions, thereby expanding their repertoire of functions (Shipman and Nicoll, 2012; Poulopoulos et al., 2012). This 'functional dimerization' property is well illustrated by the structural organization of NLGN complexes with MDGA protein 1 (for abbreviations of complicated names, or little used, see the legend to Table 2), where each of the two elongated, multi-domain MDGA molecules wraps around and bridges the two subunits in the NLGN dimer (Gangwar et al., 2017; Kim et al., 2017; Elegheert et al., 2017; Thoumine and Marchot, 2017). In contrast, superimposition of the LNS6 domain in the long

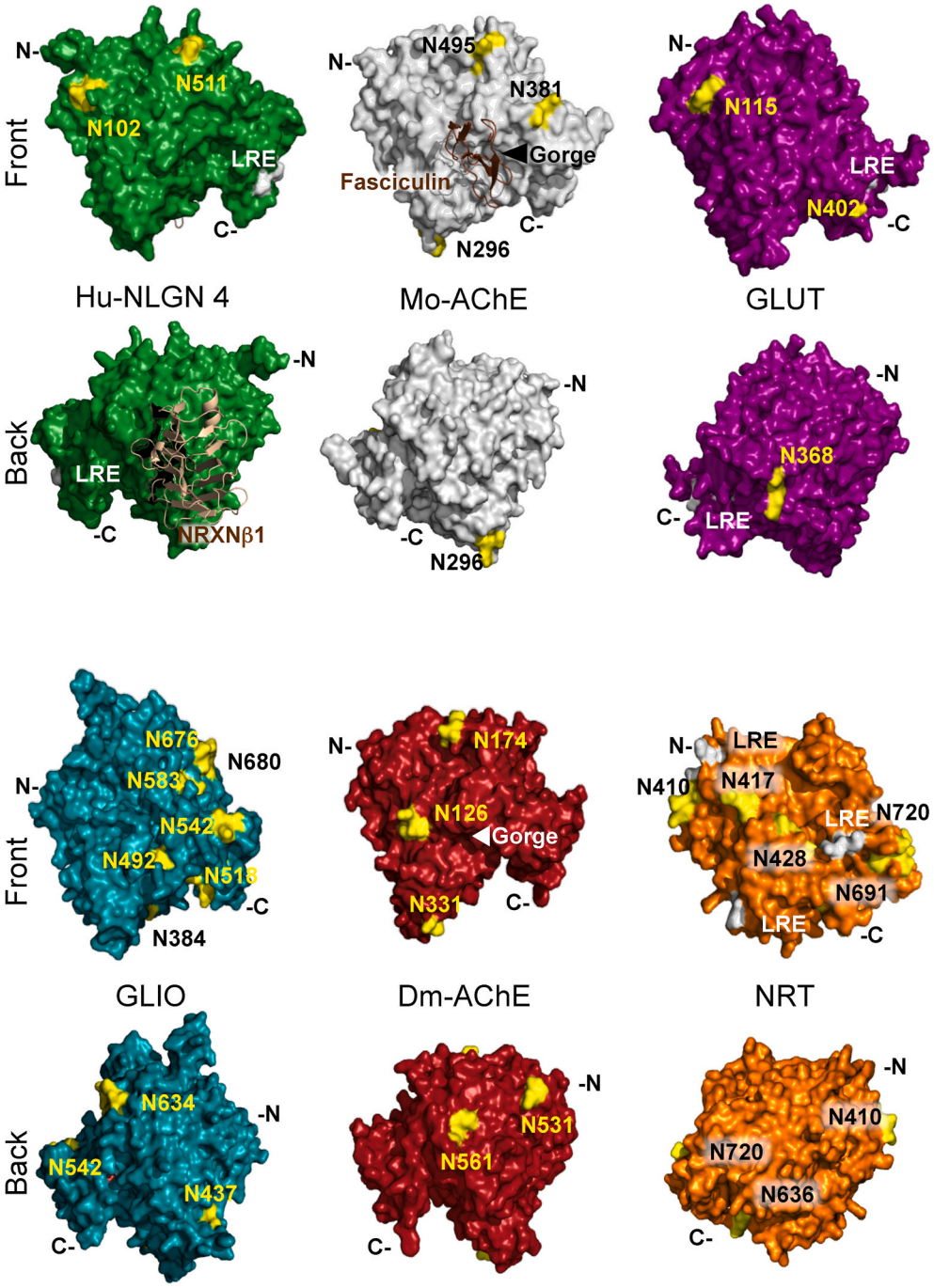

Fig. 3. – Comparative mapping of selected surface determinants on the extracellular domains of mammalian and *Drosophila* AChE and ChE-like cell-adhesion molecules - Shown are experimental structures of human NLGN4X bound with NRXNβ1 (PDB ID: 2XB6, green NLGN4X molecular surface, brown NRXNβ1 backbone ribbon), mouse AChE bound with fasciculin (1MAH, grey AChE surface, gold fasciculin ribbon) and *Drosophila* AChE (1DX4, red surface), along with homology models of *Drosophila* GLIO (blue surface), GLUT (purple surface) and NRT (orange surface). All molecules are displayed in two orientations showing the front face (where the AChE active center gorge opens, as indicated for human and *Drosophila* AChEs) and the back face (180° rotation around a vertical axis) of the subunit. Sequence-predicted positions for Asn-linked glycans are highlighted in yellow and labeled. Surface LRE motifs are highlighted in white. All N- and C-termini are labeled. Homology modeling was carried out by submitting individual protein sequences to the Swiss Model server (https://swissmodel.expasy.org/). Selected templates were: for NRT, human liver carboxylesterase 1 (PDB ID: 5A7H; 24.5% sequence identity; 93% coverage); for GLUT, *Manduca sexta* juvenile hormone esterase (2FJ0; 25.9% sequence identity; 87% coverage; for GLIO, mouse NLGN2 (3BL8; 36.2% sequence identity; 74% coverage). Figure generated with PyMol (The PyMol Molecular Graphics System, version 2.2.3, Schrödinger, LLC). For NRT, GLIO and GLU the positions of the surface loops and determinants are likely to be biased by the selected template.

NRXNα molecule, which displays a L-shape with a flexible LNS5-LNS6 hinge (Miller et al., 2011; Chen et al., 2011), onto the LNS6 domain of each of the two short NRXNβ molecules bound to a NLGN dimer, suggested that the LNS4 domain in NRXNα could act as a secondary binder to the *same* subunit as already bound with LNS6.

Whether the invertebrate ChE-like molecules form dimers is not documented. However, sequence analysis do not reveal particular features that would drastically preclude subunit association, while our homology models suggest that despite their variable length and residue composition, the two canonical α-helices, α3(7,8) and α10, are conserved and appropriately positioned for bundle formation (Figs. 1, 3 and 4). Formation of NRT dimers might either challenge or regulate its interaction with amalgam, itself shown to form a concentration-dependent dimer *in vitro* (Zeev-Ben-Mordehai et al., 2009a; 2009b). Contribution of GLIO to the architecture of tricellular junctions through direct or indirect interaction with the large, triple-repeat extracellular domain of the transmembrane protein, anakonda (Byri et al., 2015), may suggest the need for a trimeric, rather than dimeric, assembly of subunits.

3.4. Diversified N-glycosylation patterns

Consistent with their eukaryotic origin and extracellular localization, the extracellular domains of the ChE-like cell-adhesion molecules display a variable number of consensus sequences (aka sequons) for N-linked glycosylation (Fig. 1). Human NLGNs have two (conserved) to four of them (four in NLGN1, of which one in splice insert B; three in NLGN2; two in NLGN3; two in NLGN4X/Y). For the *Drosophila* proteins,

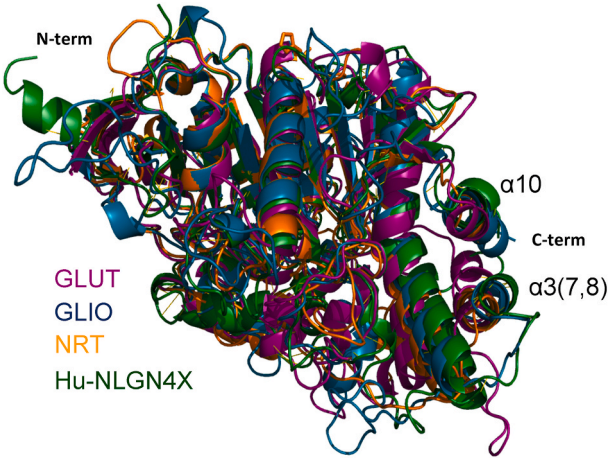

Fig. 4. – Superimposition of the homology models of NRT, GLIO, GLUT with the experimental structure of human NLGN4X. The molecule backbones are displayed as ribbons (green NLGN4X, blue GLIO, purple GLUT, orange NRT). The N- and C-termini and helices α3(7,8) and α10 are labeled. The presence of the two helices α3(7,8) and α10 is compatible with dimer formation by all of these proteins.

one finds four to six of them in the NLGNs (five in NLGNs 1–2; six in NLGN3; four in NLGN4), six in NRT, eight in GLIO, and three in GLUT, pointing to an overall greater number of sites for the insect proteins. Only for recombinant NLGNs have actual N-glycosylation patterns been characterized, either *in vitro* for rat NLGN1 (Hoffman et al., 2004) or *in cristallo* for rat/mouse NLGN1 (Araç et al., 2007; Chen et al., 2008), mouse/rat/human NLGN2 (Koehnke et al., 2008; Gangwar et al., 2017; Kim et al., 2017), and human NLGN4X (Fabrichny et al., 2007).

Comparative mapping of these sites at the surface of the respective protein structures and models (Fig. 3) points to preferential clustering on the front face, i.e., the face of the subunit where in AChE, the active center gorge opens (Ω-loop/Cys-loop face) and the inhibitory snake toxin fasciculin binds (Bourne et al., 1995; Harel et al., 1995). Fewer sites, including the one in splice insert B in rodent NLGN1 (see Fig. 1, but not shown in Fig. 3), are located on the back face, i.e., the opposite face of the subunit where in the NLGNs, NRXNβ1 or MDGA-Ig1 bind. Some of these sites appear to be fairly conserved in both the ChEs and ChE-like molecules, such as those located close to the N-terminus, just before the first Cys in disulfide bond 1 (exemplified by N102 in human NLGN4X, N115 in GLUT, N417 in NRT); within the surface loop tied by bond 2 (N296 in human AChE, N331 in *Drosophila* AChE); and close to the putative dimerization interface, just after the second Cys in bond 3b (N511 in human NLGN4, N595 in human AChE), while all were shown to be occupied, two features suggesting a structural or protective role. In NRT, five of the six sites form a weawing line across the front face, from the N- to the C-terminal corners of the subunit (Fig. 3). Overall N-glycosylation of NRT was experimentally demonstrated *in vitro*, but not the exact pattern of site occupancy (de la Escalera et al., 1990), nor N-glycan contribution to amalgam binding.

3.5. LRE motifs

The tripeptide leucine-arginine glutamate (LRE) was primarily identified as an adhesive site for s-laminin, an extracellular matrix protein influencing cell differentiation, migration and adhesion in striated muscles and peripheral nerves (Durbeej, 2010). AChE was found to bind laminin using yeast two-hybrid screening and co-immuno precipitation (Paraoanu & Layer, 2004, 2005). The positions of LRE motifs in ChEs, other enzyme relatives, and the ChE-like proteins were ranked using sequence comparison and 3D homology modeling based on AChE templates (no NLGN structures were available) and found to be distributed into four main sites at the surface of the ChE-like subunit (Johnson and Moore, 2013). Most AChEs and NLGNs along with NRT, GLIO and GLUT contain one to several complete or incomplete LRE motifs (Fig. 1), of which some indeed share similar spatial positions (Fig. 3). In mammalian NLGNs, one motif is conserved in helix α3(7,8), which contributes to the dimer interface (H1 helix in Fig. 1) (Figs. 3 and 4). In human NLGN3, the Arg residue in this particular motif is the one whose Cys substitution results in intracellular retention of a misfolded protein (De Jaco et al., 2012). In turn, both the Arg and Glu residues in this motif form an integral part of the MDGA1-Ig2 binding site on human/rat NLGNs 1 and 2 (Kim et al., 2017; Gangwar et al., 2017; Elegheert et al., 2017). These two features offer insightful functional correlation for LRE motifs in ChE-like proteins. However, none of these motifs are involved in fasciculin binding to AChE nor NRXNβ1 binding to NLGNs (Fig. 3), and whether these motifs in the ChEs or the ChE-like cell-adhesion molecules bind laminin is not documented. Still, it is noteworthy that on NRT, the first LRE motif, located at the very N-terminal end of the subunit and surrounded by two putative N-glycosylation sites (of which one is likely to be occupied, see Fig. 1), belongs to that same lobe of the subunit as shown to be mandatory for both binding of amalgam and cell-adhesion.

3.6. Calcium binding

Fasciculin binding to the peripheral anionic site of AChE, located at the entrance of the active center gorge (Fig. 3), is challenged by calcium (Karlsson et al., 1984; Marchot et al., 1993), and AChE is protected by magnesium against thermal denaturation (Millard et al., 2003). NRNX binding to NLGN is calcium-dependent (Ichtchenko et al., 1995, 1996; Comoletti et al., 2003). And GLUT binds calcium, preferably in presence of excess magnesium (Olson et al., 1990). Based on these observations, an *in silico* study pointed to putative calcium-binding motifs at the surface of ChE and ChE-like proteins (Tsigelny et al., 2000). However, no specifically bound calcium or magnesium was found in structures of AChE despite their presence in the crystallization liquors (P. Marchot, personal data), consistent with their low affinity for the peripheral site (Marchot et al., 1993), nor in a structure of NLGN4 crystallized in the presence of calcium (Fabrichny et al., 2007). In turn, calcium molecules found to be trapped at the NRXNβ1-NLGN1/4 complex interface were coordinated by NRXNβ1, with no direct interaction with the NLGN (Fabrichny et al., 2007; Araç et al., 2007; Chen et al., 2008; Leone et al., 2010). Calcium was found not to be required for MDGA binding to NLGN in solution nor in the crystal state (Kim et al., 2007; Gangwar et al., 2017; Elegheert et al., 2017).

3.7. Electrostatic surface potentials

The AChE subunit is characterized by a markedly asymmetric distribution of charged residues at its surface, generating a negatively charged face, essentially contributed by the peripheral anionic site at the entrance of the active center gorge (and identified as the Ω-loop face, or 'front face' in Fig. 3), and a positively charged face on the opposite face of the subunit (identified as the 'back face' in Fig. 3) (Sussman et al., 1991; Ripoll et al., 1993) (Fig. 5). This electrostatic pattern produces a significant dipole moment, with a vector roughly oriented along the axis of the active-site gorge, and suggested to enhance long-distance attraction of cationic substrates toward the gorge entrance and their diffusion toward the active center (Silman and Sussman, 2008). The electronegative potential of the front face of AChE was also shown to be instrumental for long-range attraction of peptidic cationic non-competitive inhibitors (such as fasciculin, see Fig. 3) toward the peripheral anionic site of the enzyme (Bourne et al., 1995, 2015; Harel et al., 1995). Early homology modeling of the extracellular domains of mouse NLGN1 and *Drosophila* NRT and GLIO, along with quantitative analysis of the electrostatic properties of their front face, evidenced a negatively charged annular patch similar to that found on *Torpedo* AChE, and led to nicknaming these proteins 'electrotactins' (Botti et al., 1998). Later on, the

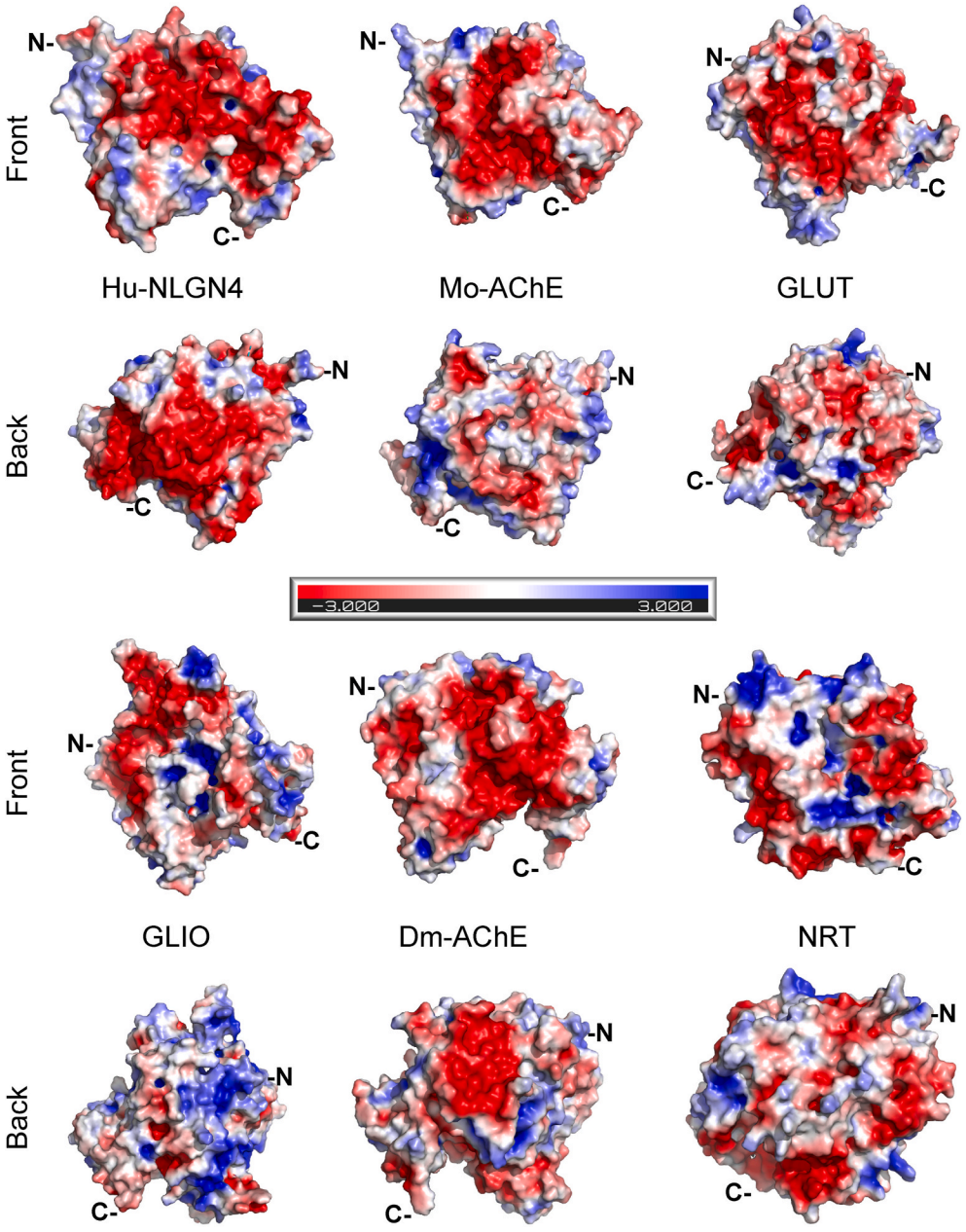

Fig. 5. – Electrostatic surface potentials of mammalian and *Drosophila* AChE and ChE-like cell-adhesion molecules. Shown are the same crystal structures of mammalian and *Drosophila* AChE and homology models of NLGN4X and *Drosophila* NRT, GLIO, GLUT, displayed in the same two orientations, as in Fig. 3. Surface potentials are expressed as a spectrum ranging from −3 kT/e (deep red) through 0 kT/e (white) to +3 kT/e (deep blue). The calculation used default parameters. Figure generated with PyMol (The PyMol Molecular Graphics System, version 2.2.3, Schrödinger, LLC). For NRT, GLIO and GLUT the positions of the surface loops and determinants are likely to be biased by the selected template.

crystal structure of human NLGN4X confirmed the electronegative character of the front face of the NLNG subunit, yet it also revealed the electronegative character of its opposite, back face (where NRXNβ1 binds, see Fig. 3), a feature generating an electronegative belt around the subunit and precluding formation of a dipole (Fabrichny et al., 2007; Leone et al., 2010) (Fig. 5).

To extend this analysis, we explored the electrostatic surface potentials of *Drosophila* AChE and rodent NLGNs 1 and 2, based on their experimental structures (Harel et al., 2000; Araç et al., 2007; Koehnke et al., 2008), and of *Drosophila* NRT based on our homology model, comparatively with those of mouse AChE and human NLGN4X, used as references (Fig. 5). Consistent with the situation with *Torpedo* AChE (see above), on mouse AChE the electronegative surface potential is restricted to the front face of the subunit, while the back face is rather positively charged. In *Drosophila* AChE, the overall electronegative character of the front face is retained but not the electropositive character of the back face, which instead presents a well-delimited, strongly electronegative patch likely to alter the dipole vector and moment found in the *Torpedo* and mouse enzymes. In NLGNs 1 and 2 the situation is similar to that found for human NLGN4X, albeit with a smaller, slightly eccentric electronegative patch on the front face of NLGN2 (data not shown). Of the three other ChE-like cell-adhesion molecules, GLUT resembles more mouse AChE for both faces of the subunit, a feature suggesting existence of a diplolar moment. In contrast, on GLIO the electronegative patch on the front face is smaller and restricted to the N-terminal part of the subunit, while the back face is frankly electropositive. It is noteworthy that on the front face, the electropositive surface area positive correlates well with the surface area devoid of N-glycan (Fig. 3). Finally, on NRT the electronegative patch on the front face appears to be split into two parts, while the back face resembles

Table 2
Identified and putative extracellular partners of the ChEs and ChE-like proteins, and their constitutive domains.

ChE or ChE-like protein	Partner	Domain type	Fold description
AChEs	Fasciculins	Three-fingered toxin	Reticulated core, central β-sheet, three emerging loops
	Antibodies	Immunoglobulin (Ig)	Two-layer sandwich of two β-sheets in a Greek key topology
	Laminin	Laminin	Central α-chain with a varying number of globular regions; β- and γ-chains with α-helical and globular regions
	Amyloid β-peptide	Helix-loop-helix	Disordered loop tied by two flanking α-helices
NLGNs	NRXNs β	LNS	β-Sandwich of 10–15 β-strands with a jelly-roll topology and canonical calcium binding sites located on one edge
	NRXNs α	(*) 3x[LNS-EGF-LNS] *(aka 'NRXN repeats')*	LNS: see above; EGF: two-stranded β-sheets separated by a loop
	MDGAs	(*) [6xIg-like]-FN3-MAM	Ig: see above; FN3: β-sandwich of two antiparallel β-sheets; MAM: compact β-sandwich of β-strands with a jelly-roll topology
	PTPRT	(*) MAM-Ig-like-[4xFN3-like]	MAM, Ig, FN3: see above
	TSP1	(*) LNS-vWFC-[3xTSP1]-[3xEGF]-[13xARCBT3R]-LTL	LNS, EGF: see above; vWFC: cystine knot (knottin) fold, i.e.,compact core of 3–4 β-strands with alternating orientation, tied by 3 disulfides; TSP1: three β-strands with alternating orientation, stabilized by disulfides; ARCBT3R: Asp-rich calcium-binding type-3 repeat; LTL: β-sandwich of two twisted antiparallel β-sheets (a variation of the jelly roll fold)
	GluN1	2xclamshell-like	Two lobes with an α/β topology tethered by a flexible 'hinge' that defines a central groove/cleft
NRT	Amalgam	3xIg-like	V-type, C2-type 1, C2-type 2
GLIO	Anakonda	(*) 3x[SRCR-like-CUB (-like)-α-helix]	SRCR-like: six stranded β-sheet and one α-helix; CUB: β-sandwich with a jelly-roll fold
GLUT	–	–	–

Abbreviations and names of domains - CUB, complement/UEGF/BMP1; EGF, Epidermal Growth Factor; FN3, FibroNectin type-III; Ig, Immunoglobuline; LNS, Laminin, Neurexin, Sex-hormone binding globulin; MAM, meprin, A-5 protein, and receptor protein-tyrosine phosphatase Mu; MDGA, Meprin, A-5 protein, and receptor protein-tyrosine phosphatase mu [MAM] Domain-containing Glycosylphosphatidylinositol Anchor; PTPRT, Receptor-type tyrosine-protein phosphatase T; SRCR, scavenger-receptor; TSP1, thrombospondin-1; vWFC, von Willebrand factor type-C; LTL, L-type lectin-like; GluN1, GluN1 subunit of the *N*-Methyl-*d*-aspartate [NMDA] receptor.
(*) From the N- to the C-terminal.

those of mouse AChE and GLUT. However, whether these features are related to partner recognition by these three cell-adhesion molecules is unknown.

4. Extracellular binding partners of the AChEs and ChE-like cell-adhesion molecules

Peptidic ChE partners with a well-documented mode of binding and action comprise two types of molecules rich in β-strands: the natural snake toxins fasciculins and three non-natural monoclonal antibodies, all acting as non-competitive AChE inhibitors (Bourne et al., 1995, 2013, 2015; Harel et al., 1995; and references in them) (Table 2). The fasciculins and two of the antibodies are cationic molecules that bind the peripheral anionic site on the front face of the enzyme, thereby occluding the entrance to the active center gorge (Fig. 3). Other proposed peptidic partners, albeit not inhibitors, of AChEs comprise laminin, a large heterotrimeric glycoprotein and a major extracellular matrix component of the basal lamina (Paraoanu & Layer 2004, 2005), and the amyloid β-peptide, whose assembly into Alzheimer's fibrils was shown to be accelerated by AChE (Inestrosa et al., 2008). Both were suggested to bind the peripheral anionic site of the enzyme. Structural analysis of mouse AChE pointed to resemblance of the amyloid β-peptide in its soluble, non-pathogenic state, with the short surface loop tied by the second disulfide bond and conserved among the ChE and ChE-like proteins (see above, and Fig. 1), thereby suggesting a mode of β-peptide nucleation by AChE to promote aggregation (Bourne et al., 1999).

Most of the identified or proposed partners of the ChE-like cell-adhesion molecules also encompass globular domains rich in β-strands, belonging to a large variety of structural families, and whose association in various combinations often forms elongated molecules (Bourne and Marchot 2014). The membrane-anchored NLGN partners, NRXNs α and β, have different extracellular domains. The extracellular domain of the long NRXNs α comprises three 'NRXN repeats' made of one LNS, one EGF and one LNS domain, while that of the short NRXNs β contains only the C-terminal, sixth LNS domain of NRXNs α (Ushkaryov et al., 1992) (Table 2). The membrane-anchored MDGAs, which belong to the immunoglobulin superfamily of proteins, comprise six Ig-like domains followed by one FN3-like domain and one MAM domain before the glycosylphosphatidylinositol anchor to the membrane (Litwack et al., 2004). In the NRNXs, only LNS6 appears to interact with NLGN, through loops forming the edge of the β-sandwich and the calcium cage (Fabrichny et al., 2007; Araç et al., 2007; Chen et al., 2008; Leone et al., 2010; Tanaka et al., 2012). For the MDGAs, these are the three consecutive Ig1-Ig2-Ig3 domains that interact with NLGN, with complementary contributions from both β-strands and intervening loops (Kim et al., 2017; Gangwar et al., 2017; Elegheert et al., 2017).

The NLGNs have also been proposed to interact extracellularly with other extracellular proteins or domains belonging to various structural families (Table 2). Of these, selective interaction of NLGNs with the transmembrane PTPRT proteins was suggested to occur with varying affinities depending on the NLGN isoform (Lim et al., 2009). This interaction appears to regulate neuronal synapse formation, consistently with the role of several PTPRTs in the control of axonal outgrowth, guidance, and synapse formation in the central nervous system. Structurally, the PTPRT extracellular domain resembles that of MDGA besides a distinct organization (Alonso et al., 2004). Co-immunoprecipitation in heterologous cells suggested that NLGN1-3 interact with TSP1 to mediate its synaptogenic effect, similar to that of NRXNs, on neuron development (Xu et al., 2010). TSP1 proteins are secreted molecules consisting of an LNS domain followed by a vWFC domain, three consecutive TSP1 repeats, three consecutive EGF-like domains, 13 Asp-rich calcium-binding type-3 repeats, and a L-type lectin-like domain (Tan et al., 2006; Misenheimer et al., 2000). The extracellular domain of NLGN1 was also reported to specifically mediate *cis* interactions with the extracellular domain of the GluN1 subunit of the NMDA receptor (Budreck et al., 2013). This GluN1 extracellular domain consists of two

large globular clamshell-like domains: an N-terminal domain involved in subunit assembly and an agonist-binding domain that binds glycine (Paoletti, 2011). Finally, the bridging of NLGN1 containing insert B with NRXNα1 (two isoforms that do not interact directly with each other, due to the steric hindrance generated by the N-glycan that caps the insert (Boucard et al., 2005) (Fig. 1)) via the astrocyte-secreted synaptogenic protein, hevin (aka SPARCL1), was suggested to contribute to the assembly of glutamatergic synapses (Singh et al., 2016). Hevin, a N- and O-glycosylated protein, contains three domains with specific structural organisations that are implicated in the regulation of cell adhesion, migration, and proliferation (Girard and Springer, 1995). However, a more recent study provided evidence that the hevin mode of action is independent of NLGNs and NRXNs (Gan and Südhof, 2020).[3]

The NRT partner, amalgam, a secreted member of the immunoglobulin superfamily, is made of three different types of Ig-like domains (Frémion et al., 2000) (Table 2). Biophysical and low-resolution structural data in solution pointed to an elongated monomer at low concentration but a V-shaped, N-terminally coordinated dimer at high concentration (Zeev-Ben-Mordehai et al., 2009a; 2009b), similar to dimers formed by neuronal IgLON proteins (Ranaivoson et al., 2019). This observation led to propose that the two amalgam arms would bind the extracellular domains of two NRT molecules respectively anchored to facing membranes, thereby promoting neurotactin clustering in *trans*, and leading to cell adhesion and axon fasciculation in *Drosophila* (Zeev-Ben-Mordehai et al., 2009b).

The putative GLIO partner, anakonda, is a transmembrane protein whose extracellular domain is made of three repeats, each comprising a SRCR-like domain, a CUB or CUB-like domain and a single-stranded right-handed β-helix motif (Byri et al., 2015) (Table 2). The unusual tripartite organization of this domain was suggested to be correlated to requirement of anakonda for the formation of tricellular, but not bicellular junctions (Byri et al., 2015). Synergistic contribution by the four-transmembrane domain, proteolipid protein M6 was recently reported (Esmangart de Bournonville and Le Borgne, 2020; Wittek et al., 2020).

No specific binding partner for GLUT has been identified. However, protein-protein associations involving a large number of individual *Drosophila* proteins, examined using co-affinity purification coupled to mass spectrometry analysis, pointed to more than 30 potential interaction partners belonging to various protein types and families (Guruharsha et al., 2011). These data now await independent validation.

5. Conclusion

ChE-like cell-adhesion molecules play a role during the development of multiple tissues within a wide range of metazoans. This small subset of the α/β-hydrolase superfamily of proteins shares an extracellular or soluble domain structurally related to the catalytic domain of the ChE enzymes, but they lost catalytic properties and aquired heterophilic partner recognition and association functions during evolution. This evolutionary divergence included variations in the disulfide bonding; in the presence, number and position of particular loops, N-glycans and repeat motifs and in the repartition of electrostatic charges at the surface of the molecule; and possibly in dimer formation. The NLGNs have been extensively studied at the functional and structural levels and several extracellular binding partners have been either identified and characterized, or proposed. A NRT binding partner has been identified and characterized; yet their mode of association and resulting mode of action remain unclear. For GLIO and GLUT, no *bona fide* endogenous ligands or receptors have been identified. Documenting and comparing the structure-function relationships of these partnerships is instrumental to understand how they work at the cellular level. Moreover, this knowledge is critical to expand our understanding of surface determinants for cell-adhesion and try to assign cell-adhesion functions to poorly characterized ChE-like proteins with an altered active-center machinery.

[3] Sentence and reference added after this article was accepted for publication.

Funding

This work was funded in part by the RWJ Foundation grant #74260 and strategic research funds from the School of Biological Sciences at Victoria University of Wellington (to D.C.), and by the CNRS and Aix-Marseille Univ (to Y.B. and P.M.).

Author contributions

DC: Conceptualization; Data curation; Formal analysis; Funding acquisition; Project administration; Supervision; Validation; Visualization; Writing - original draft, review, editing.
LT: Conceptualization; Data curation; Formal analysis; Validation; Visualization; Writing - original draft, review, editing.
AC: Data curation; Formal analysis; Writing – review, editing.
YB: Formal analysis; Visualization.
PM: Conceptualization; Data curation; Formal analysis; Project administration; Supervision; Validation; Visualization; Writing - original draft, review, editing.

Declaration of competing interest

The authors declare no conflict of interest.

References

Alonso, A., Sasin, J., Bottini, N., Friedberg, Ilan, Friedberg, Iddo, Osterman, A., Godzik, A., Hunter, T., Dixon, J., Mustelin, T., 2004. Protein tyrosine phosphatases in the human genome. Cell 117, 699–711. https://doi.org/10.1016/j.cell.2004.05.018.

Apóstolo, N., de Wit, J., 2019. Compartmentalized distributions of neuronal and glial cell-surface proteins pattern the synaptic network. Curr. Opin. Neurobiol. 57, 126–133. https://doi.org/10.1016/j.conb.2019.01.025.

Araç, D., Boucard, A.A., Özkan, E., Strop, P., Newell, E., Sudhöf, T.C., Brunger, A.T., 2007. Structures of neuroligin-1 and the neuroligin-1/neurexin-1β complex reveal specific protein-protein and protein-Ca2+ interactions. Neuron 56, 992–1003. https://doi.org/10.1016/j.neuron.2007.12.002.

Auld, V.J., Fetter, R.D., Broadie, K., Goodman, C.S., 1995. Gliotactin, a novel transmembrane protein on peripheral glia, is required to form the blood-nerve barrier in Drosophila. Cell 81, 757–767. https://doi.org/10.1016/0092-8674(95)90537-5.

Bakian, A.V., VanDerslice, J.A., 2019. Pesticides and autism. BMJ l1149. https://doi.org/10.1136/bmj.l1149.

Barthalay, Y., Hipeau-Jacquotte, R., de la Escalera, S., Jiménez, F., Piovant, M., 1990. Drosophila neurotactin mediates heterophilic cell adhesion. EMBO J. 9, 3603–3609.

Bolliger, M.F., Frei, K., Winterhalter, K.H., Gloor, S.M., 2001. Identification of a novel neuroligin in humans which binds to PSD-95 and has a widespread expression. Biochem. J. 356, 581–588. https://doi.org/10.1042/0264-6021:3560581.

Bolliger, M.F., Pei, J., Maxeiner, S., Boucard, A.A., Grishin, N.V., Südhof, T.C., 2008. Unusually rapid evolution of Neuroligin-4 in mice. Proc. Natl. Acad. Sci. U.S.A. 105, 6421–6426. https://doi.org/10.1073/pnas.0801383105.

Botti, S.A., Felder, C.E., Sussman, J.L., Silman, I., 1998. Electrotactins: a class of adhesion proteins with conserved electrostatic and structural motifs. Protein Eng. Des. Sel. 11, 415–420. https://doi.org/10.1093/protein/11.6.415.

Bottos, A., Destro, E., Rissone, A., Graziano, S., Cordara, G., Assenzio, B., Cera, M.R., Mascia, L., Bussolino, F., Arese, M., 2009. The synaptic proteins neurexins and neuroligins are widely expressed in the vascular system and contribute to its functions. Proc. Natl. Acad. Sci. U.S.A. 106, 20782–20787. https://doi.org/10.1073/pnas.0809510106.

Boucard, A.A., Chubykin, A.A., Comoletti, D., Taylor, P., Sudhöf, T.C., 2005. A splice code for trans-synaptic cell adhesion mediated by binding of neuroligin 1 to α- and β-neurexins. Neuron 48, 229–236. https://doi.org/10.1016/j.neuron.2005.08.026.

Bourne, Y., Grassi, J., Bougis, P.E., Marchot, P., 1999. Conformational flexibility of the acetylcholinesterase tetramer suggested by x-ray crystallography. J. Biol. Chem. 274, 30370–30376. https://doi.org/10.1074/jbc.274.43.30370.

Bourne, Y., Marchot, P., 2014. The neuroligins and their ligands: from structure to function at the synapse. J. Mol. Neurosci. 53, 387–396. https://doi.org/10.1007/s12031-014-0234-6.

Bourne, Y., Marchot, P., 2017. Hot spots for protein partnerships at the surface of cholinesterases and related α/β hydrolase fold proteins or domains - a structural perspective. Molecules 23, 35. https://doi.org/10.3390/molecules23010035.

Bourne, Y., Renault, L., Essono, S., Mondielli, G., Lamourette, P., Boquet, D., Grassi, J., Marchot, P., 2013. Molecular characterization of monoclonal antibodies that inhibit

acetylcholinesterase by targeting the peripheral site and backdoor region. PloS One 8, e77226. https://doi.org/10.1371/journal.pone.0077226.

Bourne, Y., Renault, L., Marchot, P., 2015. Crystal structure of snake venom acetylcholinesterase in complex with inhibitory antibody fragment Fab410 bound at the peripheral site: evidence for open and closed states of a back door channel. J. Biol. Chem. 290, 1522–1535. https://doi.org/10.1074/jbc.M114.603902.

Bourne, Y., Taylor, P., Marchot, P., 1995. Acetylcholinesterase inhibition by fasciculin: crystal structure of the complex. Cell 83, 503–512. https://doi.org/10.1016/0092-8674(95)90128-0.

Budreck, E.C., Kwon, O.-B., Jung, J.H., Baudouin, S., Thommen, A., Kim, H.-S., Fukazawa, Y., Harada, H., Tabuchi, K., Shigemoto, R., Scheiffele, P., Kim, J.-H., 2013. Neuroligin-1 controls synaptic abundance of NMDA-type glutamate receptors through extracellular coupling. Proc. Natl. Acad. Sci. U.S.A. 110, 725–730. https://doi.org/10.1073/pnas.1214718110.

Budreck, E.C., Scheiffele, P., 2007. Neuroligin-3 is a neuronal adhesion protein at GABAergic and glutamatergic synapses. Eur. J. Neurosci. 26, 1738–1748. https://doi.org/10.1111/j.1460-9568.2007.05842.x.

Byri, S., Misra, T., Syed, Z.A., Bätz, T., Shah, J., Boril, L., Glashauser, J., Aegerter-Wilmsen, T., Matzat, T., Moussian, B., Uv, A., Luschnig, S., 2015. The triple-repeat protein anakonda controls epithelial tricellular junction formation in Drosophila. Dev. Cell 33, 535–548. https://doi.org/10.1016/j.devcel.2015.03.023.

Cao, X., Tabuchi, K., 2017. Functions of synapse adhesion molecules neurexin/neuroligins and neurodevelopmental disorders. Neurosci. Res. 116, 3–9. https://doi.org/10.1016/j.neures.2016.09.005.

Carr, P.D., Ollis, D.L., 2009. α/βHydrolase fold: an update. Protein Pept. Lett. 16, 1137–1148. https://doi.org/10.2174/092986609789071298.

Chatonnet, A., Brazzolotto, X., Hotelier, T., Lenfant, N., Marchot, P., Bourne, Y., 2019. An evolutionary perspective on the first disulfide bond in members of the cholinesterase-carboxylesterase (COesterase) family: possible outcomes for cholinesterase expression in prokaryotes. Chem. Biol. Interact. 308, 179–184. https://doi.org/10.1016/j.cbi.2019.05.016.

Chen, F., Venugopal, V., Murray, B., Rudenko, G., 2011. The structure of neurexin 1alpha reveals features promoting a role as synaptic organizer. Structure 19, 779–789. https://doi.org/10.1016/j.str.2011.03.012.

Chen, X., Liu, H., Shim, A.H.R., Focia, P.J., He, X., 2008. Structural basis for synaptic adhesion mediated by neuroligin-neurexin interactions. Nat. Struct. Mol. Biol. 15, 50–56. https://doi.org/10.1038/nsmb1350.

Cheung, J., Mahmood, A., Kalathur, R., Liu, L., Carlier, P.R., 2018. Structure of the G119S mutant acetylcholinesterase of the malaria vector Anopheles gambiae reveals basis of insecticide resistance. Structure 26, 130–136. https://doi.org/10.1016/j.str.2017.11.021.

Chih, B., Afridi, S.K., Clark, L., Scheiffele, P., 2004. Disorder-associated mutations lead to functional inactivation of neuroligins. Hum. Mol. Genet. 13, 1471–1477. https://doi.org/10.1093/hmg/ddh158.

Chih, B., Gollan, L., Scheiffele, P., 2006. Alternative splicing controls selective trans-synaptic interactions of the neuroligin-neurexin complex. Neuron 51, 171–178. https://doi.org/10.1016/j.neuron.2006.06.005.

Comoletti, D., 2004. The Arg451Cys-neuroligin-3 mutation associated with autism reveals a defect in protein processing. J. Neurosci. 24, 4889–4893. https://doi.org/10.1523/JNEUROSCI.0468-04.2004.

Comoletti, D., Flynn, R., Jennings, L.L., Chubykin, A., Matsumura, T., Hasegawa, H., Südhof, T.C., Taylor, P., 2003. Characterization of the interaction of a recombinant soluble neuroligin-1 with neurexin-1β. J. Biol. Chem. 278, 50497–50505. https://doi.org/10.1074/jbc.M306803200.

Comoletti, D., Flynn, R.E., Boucard, A.A., Demeler, B., Schirf, V., Shi, J., Jennings, L.L., Newlin, H.R., Südhof, T.C., Taylor, P., 2006. Gene selection, alternative splicing, and post-translational processing regulate neuroligin selectivity for β-neurexins. Biochemistry 45, 12816–12827. https://doi.org/10.1021/bi0614131.

Comoletti, D., Grishaev, A., Whitten, A.E., Tsigelny, I., Taylor, P., Trewhella, J., 2007. Synaptic arrangement of the neuroligin/β-neurexin complex revealed by x-ray and neutron scattering. Structure 15, 693–705. https://doi.org/10.1016/j.str.2007.04.010.

Daoud, H., Bonnet-Brilhault, F., Védrine, S., Demattéi, M.-V., Vourc'h, P., Bayou, N., Andres, C.R., Barthélémy, C., Laumonnier, F., Briault, S., 2009. Autism and nonsyndromic mental retardation associated with a de novo mutation in the nlgn4x gene promoter causing an increased expression level. Biol. Psychiatr. 66, 906–910. https://doi.org/10.1016/j.biopsych.2009.05.008.

De Jaco, A., Comoletti, D., Dubi, N., Camp, S., Taylor, P., 2012. Processing of cholinesterase-like α/β-hydrolase fold proteins: alterations associated with congenital disorders. Protein Pept. Lett. 19, 173–179. https://doi.org/10.2174/092986612799080103.

De Jaco, A., Comoletti, D., Kovarik, Z., Gaietta, G., Radić, Z., Lockridge, O., Ellisman, M. H., Taylor, P., 2006. A mutation linked with autism reveals a common mechanism of endoplasmic reticulum retention for the α,β-hydrolase fold protein family. J. Biol. Chem. 281, 9667–9676. https://doi.org/10.1074/jbc.M510262200.

de la Escalera, S., Bockamp, E.O., Moya, F., Piovant, M., Jiménez, F., 1990. Characterization and gene cloning of neurotactin, a Drosophila transmembrane protein related to cholinesterases. EMBO J. 9, 3593–3601.

de Wit, J., Ghosh, A., 2016. Specification of synaptic connectivity by cell surface interactions. Nat. Rev. Neurosci. 17 https://doi.org/10.1038/nrn.2015.3, 4-4.

Dong, N., Qi, J., Chen, G., 2007. Molecular reconstitution of functional GABAergic synapses with expression of neuroligin-2 and GABAA receptors. Mol. Cell. Neurosci. 35, 14–23. https://doi.org/10.1016/j.mcn.2007.01.013.

Durbeej, M., 2010. Laminins. Cell Tissue Res. 339, 259–268. https://doi.org/10.1007/s00441-009-0838-2.

Dvir, H., Silman, I., Rosenberry, T.L., Sussman, J.L., 2010. Acetylcholinesterase: from 3D structure to function. Chem. Biol. Interact. 187, 10–22. https://doi.org/10.1016/j.cbi.2010.01.042.

Elegheert, J., Cvetkovska, V., Clyton, A.J., Heroven, C., Vennekens, K.M., Smukowski, S. N., Regan, M.C., Jia, W., Smith, A.C., Furukawa, H., Savas, J.N., de Wit, J., Begbie, J., Craig, A.M., Aricescu, A.R., 2017. Structural mechanism for modulation of synaptic neuroligin-neurexin signaling by MDGA proteins. Neuron 95, 896–913. https://doi.org/10.1016/j.neuron.2017.07.040.

Esmangart de Bournonville, T., Le Borgne, R., 2020. Interplay between anakonda, gliotactin, and M6 for tricellular junction assembly and anchoring of septate junctions in Drosophila epithelium. Curr. Biol. 30, 4245–4253.e4. https://doi.org/10.1016/j.cub.2020.07.090.

Fabrichny, I.P., Leone, P., Sulzenbacher, G., Comoletti, D., Miller, M.T., Taylor, P., Bourne, Y., Marchot, P., 2007. Structural analysis of the synaptic protein Neuroligin and its β-Neurexin complex: determinants for folding and cell adhesion. Neuron 56, 979–991. https://doi.org/10.1016/j.neuron.2007.11.013.

Földy, C., Malenka, R.C., Südhof, T.C., 2013. Autism-associated neuroligin-3 mutations commonly disrupt tonic endocannabinoid signaling. Neuron 78, 498–509. https://doi.org/10.1016/j.neuron.2013.02.036.

Frémion, F., Darboux, I., Diano, M., Hipeau-Jacquotte, R., Seeger, M.A., Piovant, M., 2000. Amalgam is a ligand for the transmembrane receptor neurotactin and is required for neurotactin-mediated cell adhesion and axon fasciculation in Drosophila. EMBO J. 19, 4463–4472. https://doi.org/10.1093/emboj/19.17.4463.

Gan, K.J., Südhof, T.C., 2020. SPARCL1 promotes excitatory but not inhibitory synapse formation and function independent of neurexins and neuroligins. J. Neurosci. 40, 8088–8102. https://doi.org/10.1523/JNEUROSCI.0454-20.2020.

Gangwar, S.P., Zhong, X., Seshadrinathan, S., Chen, H., Machius, M., Rudenko, G., 2017. Molecular mechanism of MDGA1: regulation of neuroligin 2:neurexin trans-synaptic bridges | Elsevier Enhanced Reader. Neuron 94, 1132–1141. https://doi.org/10.1016/j.neuron.2017.06.009.

Gilbert, M.M., Auld, V.J., 2005. Evolution of CLAMs (Cholinesterase-Like adhesion molecules): structure and function during development. Front. Biosci. 10, 2177–2192. https://doi.org/10.2741/1689.

Girard, J.P., Springer, T.A., 1995. Cloning from purified high endothelial venule cells of hevin, a close relative of the antiadhesive extracellular matrix protein SPARC. Immunity 2, 113–123. https://doi.org/10.1016/1074-7613(95)90083-7.

Graf, E.R., Zhang, X., Jin, S.-X., Linhoff, M.W., Craig, A.M., 2004. Neurexins induce differentiation of GABA and glutamate postsynaptic specializations via neuroligins. Cell 119, 1013–1026. https://doi.org/10.1016/j.cell.2004.11.035.

Grifman, M., Galyam, N., Seidman, S., Soreq, H., 1998. Functional redundancy of acetylcholinesterase and neuroligin in mammalian neuritogenesis. Proc. Natl. Acad. Sci. U.S.A. 95, 13935–13940. https://doi.org/10.1073/pnas.95.23.13935.

Grisaru, D., Sternfeld, M., Eldor, A., Glick, D., Soreq, H., 1999. Structural roles of acetylcholinesterase variants in biology and pathology. Eur. J. Biochem. 264, 672–686. https://doi.org/10.1046/j.1432-1327.1999.00693.x.

Guruharsha, K.G., Rual, J.F., Zhai, B., Mintseris, J., Vaidya, P., Beekman, C., Wong, C., Rhee, D.Y., Cenaj, O., McKillip, E., Shah, S., Stapleton, M., Wan, K.H., Yu, C., Parsa, B., Carlson, J.W., Chen, X., Kapadia, B., VijarRaghavan, K., Gygi, S.P., Celniker, S.E., Obar, R.A., Artavanis-Tsakonas, S., 2011. A protein complex network of Drosophila melanogaster. Cell 147, 690–703. https://doi.org/10.1016/j.cell.2011.08.047.

Han, Q., Wong, D.M., Robinson, H., Ding, H., Lam, P.C.H., Totrov, M.M., Carlier, P.R., Li, J., 2018. Crystal structure of acetylcholinesterase catalytic subunits of the malaria vector Anopheles gambiae. Insect Sci. 25, 721–724. https://doi.org/10.1111/1744-7917.12450.

Harel, M., Kleywegt, G.J., Ravelli, R.B., Silman, I., Sussman, J.L., 1995. Crystal structure of an acetylcholinesterase-fasciculin complex: interaction of a three-fingered toxin from snake venom with its target. Structure 3, 1355–1366. https://doi.org/10.1016/s0969-2126(01)00273-8.

Harel, M., Kryger, G., Rosenberry, T.L., Mallender, W.D., Lewis, T., Fletcher, R.J., Guss, J. M., Silman, I., Sussman, J.L., 2000. Three-dimensional structures of Drosophila melanogaster acetylcholinesterase and of its complexes with two potent inhibitors. Protein Sci. 9, 1063–1072. https://doi.org/10.1110/ps.9.6.1063.

Hoffman, R.C., Jennings, L.L., Tsigelny, I., Comoletti, D., Flynn, R.E., Sudhof, T.C., Taylor, P., 2004. Structural characterization of recombinant soluble rat neuroligin 1: mapping of secondary structure and glycosylation by mass spectrometry. Biochemistry 43, 1496–1506. https://doi.org/10.1021/bi035278t.

Hoon, M., Soykan, T., Falkenburger, B., Hammer, M., Patrizi, A., Schmidt, K.-F., Sassoè-Pognetto, M., Löwel, S., Moser, T., Taschenberger, H., Brose, N., Varoqueaux, F., 2011. Neuroligin-4 is localized to glycinergic postsynapses and regulates inhibition in the retina. Proc. Natl. Acad. Sci. U.S.A. 108, 3053–3058. https://doi.org/10.1073/pnas.1006946108.

Hortsch, M., 1997. Duplications in nomenclature. Nature 389, 539. https://doi.org/10.1038/39172.

Hortsch, M., Patel, N.H., Bieber, A.J., Traquina, Z.R., Goodman, C.S., 1990. Drosophila neurotactin, a surface glycoprotein with homology to serine esterases, is dynamically expressed during embryogenesis. Development 110, 1327–1340.

Hotelier, T., Renault, L., Cousin, X., Negre, V., Marchot, P., Chatonnet, A., 2004. ESTHER, the database of the α/β-hydrolase fold superfamily of proteins. Nucleic Acids Res. 32, D145–D147. https://doi.org/10.1093/nar/gkh141.

Ichtchenko, K., Hata, Y., Nguyen, T., UIIrich, B., Messier, M., Moomaw, C., 1995. Neuroligin 1: a splice site-specific ligand for beta-neurexins. Cell 81, 435–443. https://doi.org/10.1016/0092-8674(95)90396-8.

Ichtchenko, K., Nguyen, T., Sudhof, T.C., 1996. Structures, alternative splicing, and neurexin binding of multiple neuroligins. J. Biol. Chem. 271, 2676–2682. https://doi.org/10.1074/jbc.271.5.2676.

Inaki, M., Yoshikawa, S., Thomas, J.B., Aburatani, H., Nose, A., 2007. Wnt is a local repulsive cue that determines synaptic target specificity. Curr. Biol. 17, 1574–1579. https://doi.org/10.1016/j.cub.2007.08.013.

Inestrosa, N.C., Dinamarca, M.C., Alvarez, A., 2008. Amyloid-cholinesterase interactions. Implications for Alzheimer's disease. FEBS J. 275, 625–632. https://doi.org/10.1111/j.1742-4658.2007.06238.x.

Jamain, S., Quach, H., Betancur, C., Råstam, M., Gillberg, Carina, Soderstrom, H., Giros, B., Laboyer, M., Gillberg, Christopher, Bourgeron, T., 2003. Paris autism research international sibpair (PARIS) study. Mutations of the X-linked genes encoding neuroligins NLGN3 and NLGN4 are associated with autism. Nat. Genet. 34, 27–29. https://doi.org/10.1038/ng1136.

Johnson, G., Moore, S.W., 2013. The Leu-Arg-Glu (LRE) adhesion motif in proteins of the neuromuscular junction with special reference to proteins of the carboxylesterase/cholinesterase family. Comp. Biochem. Physiol. Genom. Proteonomics 8, 231–243. https://doi.org/10.1016/j.cbd.2013.06.001.

Kang, H.S., Lee, C.K., Kim, J.R., Yu, S.J., Kang, S.G., Moon, D.H., Lee, C.H., Kim, D.K., 2004. Gene expression analysis of the pro-oestrous-stage rat uterus reveals neuroligin 2 as a novel steroid-regulated gene. Reprod. Fertil. Dev. 16, 763–772. https://doi.org/10.1071/rd04040.

Karlsson, E., Mbugua, P.M., Rodriguez-Ithurralde, D., 1984. Fasciculins, anticholinesterase toxins from the venom of the green mamba Dendroaspis angusticeps. J. Physiol. (Paris) 79, 232–240.

Kim, A.J., Kim, D., Won, S.Y., Han, K.A., Park, D., Cho, E., Yun, N., An, H.J., Um, J.W., Lee, J.-O., Ko, J., Kim, H.M., 2017. Structural insights into modulation of neurexin-neuroligin trans-synaptic adhesion by MDGA1/neuroligin-2 complex. Neuron 94, 1121–1131. https://doi.org/10.1016/j.neuron.2017.05.034.

Koehnke, J., Jin, X., Budreck, E.C., Posy, S., Scheiffele, P., Honig, B., Shapiro, L., 2008. Crystal structure of the extracellular cholinesterase-like domain from neuroligin-2. Proc. Natl. Acad. Sci. U.S.A. 105, 1873–1878. https://doi.org/10.1073/pnas.0711701105.

Koehnke, J., Katsamba, P.S., Ahlsen, G., Bahna, F., Vendome, J., Honig, B., Jin, X., 2010. Splice form-dependence of beta-neurexin/neuroligin binding interactions. Neuron 67, 61–74. https://doi.org/10.1016/j.neuron.2010.06.001.

Krejci, E., Duval, N., Chatonnet, A., Vincens, P., Massoulie, J., 1991. Cholinesterase-like domains in enzymes and structural proteins: functional and evolutionary relationships and identification of a catalytically essential aspartic acid. Proc. Natl. Acad. Sci. U.S.A. 88, 6647–6651. https://doi.org/10.1073/pnas.88.15.6647.

Kumar, S., Stecher, G., Tamura, K., 2016. MEGA7: molecular evolutionary genetics analysis version 7.0 for bigger datasets. Mol. Biol. Evol. 33, 1870–1874. https://doi.org/10.1093/molbev/msw054.

Landini, M., Merelli, I., Raggi, M.E., Galluccio, N., Ciceri, F., Bonfanti, A., Camposeo, S., Massagli, A., Villa, L., Salvi, E., Cusi, D., Molteni, M., Milanesi, L., Marabotti, A., Mezzelani, A., 2016. Association analysis of noncoding variants in neuroligins 3 and 4X genes with autism spectrum disorder in an Italian cohort. Int. J. Mol. Sci. 17, 1765. https://doi.org/10.3390/ijms17101765.

Laumonnier, F., Bonnet-Brilhault, F., Gomot, M., Blanc, R., David, A., Moizard, M.-P., Raynaud, M., Ronce, N., Lemonnier, E., Calvas, P., Laudier, B., Chelly, J., Fryns, J.-P., Ropers, H.-H., Hamel, B.C.J., Andres, C., Barthélémy, C., Moraine, C., Briault, S., 2004. X-Linked mental retardation and autism are associated with a mutation in the NLGN4 gene, a member of the neuroligin family. Am. J. Hum. Genet. 74, 552–557. https://doi.org/10.1086/382137.

Lawson-Yuen, A., Saldivar, J.-S., Sommer, S., Picker, J., 2008. Familial deletion within NLGN4 associated with autism and Tourette syndrome. Eur. J. Hum. Genet. 16, 614–618. https://doi.org/10.1038/sj.ejhg.5202006.

Leone, P., Comoletti, D., Taylor, P., Bourne, Y., Marchot, P., 2010. Structure-function relationships of the α/β-hydrolase fold domain of neuroligin: a comparison with acetylcholinesterase. Chem. Biol. Interact. 187, 49–55. https://doi.org/10.1016/j.cbi.2010.01.030.

Lenfant, N., Hotelier, T., Bourne, Y., Marchot, P., Chatonnet, A., 2014. Tracking the origin and divergence of cholinesterases and neuroligins: the evolution of synaptic proteins. J. Mol. Neurosci. 53, 362–369. https://doi.org/10.1007/s12031-013-0194-2.

Lim, S.-H., Kwon, S.-K., Lee, M.K., Moon, J., Jeong, D.G., Park, E., Kim, S.J., Park, B.C., Lee, S.C., Ryu, S.-E., Yu, D.-Y., Chung, B.H., Kim, E., Myung, P.-K., Lee, J.-R., 2009. Synapse formation regulated by protein tyrosine phosphatase receptor T through interaction with cell adhesion molecules and Fyn. EMBO J. 28, 3564–3578. https://doi.org/10.1038/emboj.2009.289.

Litwack, E.D., Babey, R., Buser, R., Gesemann, M., O'Leary, D.D.M., 2004. Identification and characterization of two novel brain-derived immunoglobulin superfamily members with a unique structural organization. Mol. Cell. Neurosci. 25, 263–274. https://doi.org/10.1016/j.mcn.2003.10.016.

Marchot, P., Chatonnet, A., 2012. Special Issue 'Hydrolase versus other functions of members of the alpha/beta-hydrolase fold superfamily of proteins'. Protein Pept. Lett. 19, 130–197.

Marchot, P., Khélif, A., Ji, Y.H., Mansuelle, P., Bougis, P.E., 1993. Binding of ^{125}I-fasciculin to rat brain acetylcholinesterase. The complex still binds diisopropyl fluorophosphate. J. Biol. Chem. 268, 12458–12467.

Maxeiner, S., Benseler, F., Krasteva-Christ, G., Brose, N., Südhof, T.C., 2020. Evolution of the autism-associated neuroligin-4 gene reveals broad erosion of pseudoautosomal regions in rodents. Mol. Biol. Evol. 37, 1243–1258. https://doi.org/10.1093/molbev/msaa014.

Millard, C.B., Shnyrov, V.L., Newstead, S., Shin, I., Roth, E., Silman, I., Weiner, L., 2003. Stabilization of a metastable state of Torpedo californica acetylcholinesterase by chemical chaperones. Protein Sci. 12, 2337–2347. https://doi.org/10.1110/ps.03110703.

Miller, M.T., Mileni, M., Comoletti, D., Stevens, R.C., Harel, M., Taylor, P., 2011. The crystal structure of the alpha-neurexin-1 extracellular region reveals a hinge point for mediating synaptic adhesion and function. Structure 19, 767–778. https://doi.org/10.1016/j.str.2011.03.011.

Misenheimer, T.M., Huwiler, K.G., Annis, D.S., Mosher, D.F., 2000. Physical characterization of the procollagen module of human thrombospondin 1 expressed in insect cells. J. Biol. Chem. 275, 40938–40945. https://doi.org/10.1074/jbc.M007022200.

Montella, I.R., Schama, R., Valle, D., 2012. The classification of esterases: an important gene family involved in insecticide resistance - a review. Mem. Inst. Oswaldo Cruz 107, 437–449. https://doi.org/10.1590/S0074-02762012000400001.

Nakanishi, M., Nomura, J., Ji, X., Tamada, K., Arai, T., Takahashi, E., Bućan, M., Takumi, T., 2017. Functional significance of rare neuroligin 1 variants found in autism. PLoS Genet. 13, e1006940 https://doi.org/10.1371/journal.pgen.1006940.

Nei, M., Kumar, S., 2000. Molecular Evolution and Phylogenetics. Oxford University Press, New York.

Nicolet, Y., Lockridge, O., Masson, P., Fontecilla-Camps, J.C., Nachon, F., 2003. Crystal structure of human butyrylcholinesterase and of its complexes with substrate and products. J. Biol. Chem. 278, 41141–41147. https://doi.org/10.1074/jbc.M210241200.

Ollis, D.L., Cheah, E., Cygler, M., Dijkstra, B., Frolow, F., Franken, S.M., Harel, M., Remington, S.J., Silman, I., Schrag, J., Sussman, J.L., Verschueren, K.H.G., Goldman, A., 1992. The α/β hydrolase fold. Protein Eng. Des. Sel. 5, 197–211. https://doi.org/10.1093/protein/5.3.197.

Olson, P.F., Fessler, L.I., Nelson, R.E., Sterne, R.E., Campbell, A.G., Fessler, J.H., 1990. Glutactin, a novel Drosophila basement membrane-related glycoprotein with sequence similarity to serine esterases. EMBO J. 9, 1219–1227.

Pampanos, A., Volaki, K., Kanavakis, E., Papandreou, O., Youroukos, S., Thomaidis, L., Karkelis, S., Tzetis, M., Kitsiou-Tzeli, S., 2009. A substitution involving the NLGN4 gene associated with autistic behavior in the Greek population. Genet. Test. Mol. Biomarkers 13, 611–615. https://doi.org/10.1089/gtmb.2009.0005.

Paoletti, P., 2011. Molecular basis of NMDA receptor functional diversity. Eur. J. Neurosci. 33, 1351–1365. https://doi.org/10.1111/j.1460-9568.2011.07628.x.

Paraoanu, L.E., Layer, P.G., 2004. Mouse acetylcholinesterase interacts in yeast with the extracellular matrix component laminin-1β. FEBS Lett. 576, 161–164. https://doi.org/10.1016/j.febslet.2004.08.078.

Paraoanu, L.E., Layer, P.G., 2005. Mouse AChE binds in vivo to domain IV of laminin-1β. Chem. Biol. Interact. 157–158, 411–413. https://doi.org/10.1016/j.cbi.2005.10.081.

Philibert, R.A., Winfield, S.L., Sandhu, H.K., Martin, B.M., Ginns, E.I., 2000. The structure and expression of the human neuroligin-3 gene. Gene 246, 303–310. https://doi.org/10.1016/S0378-1119(00)00049-4.

Poulopoulos, A., Soykan, T., Tuffy, L.P., Hammer, M., Varoqueaux, F., Brose, N., 2012. Homodimerization and isoform-specific heterodimerization of neuroligins. Biochem. J. 446, 321–330. https://doi.org/10.1042/BJ20120808.

Quartier, A., Courraud, J., Ha, T.T., McGillivray, G., Isidor, B., Rose, K., Drouot, N., Savidan, M.-A., Feger, C., Jagline, H., Chelly, J., Shaw, M., Laumonnier, F., Gecz, J., Mandel, J.-L., Piton, A., 2019. Novel mutations in NLGN3 causing autism spectrum disorder and cognitive impairment. Hum. Mutat. 40, 2021–2032. https://doi.org/10.1002/humu.23836.

Ranaivoson, F.M., Turk, L.S., Ozgul, S., Kakehi, S., von Daake, S., Lopez, N., Trobiani, L., De Jaco, A., Denissova, N., Demeler, B., Özkan, E., Montelione, G.T., Comoletti, D., 2019. A proteomic screen of neuronal cell-surface molecules reveals IgLONs as structurally conserved interaction modules at the synapse. Structure 27, 893–906. https://doi.org/10.1016/j.str.2019.03.004.

Ripoll, D.R., Faerman, C.H., Axelsen, P.H., Silman, I., Sussman, J.L., 1993. An electrostatic mechanism for substrate guidance down the aromatic gorge of acetylcholinesterase. Proc. Natl. Acad. Sci. U.S.A. 90, 5128–5132. https://doi.org/10.1073/pnas.90.11.5128.

Saitou, N., Nei, M., 1987. The neighbor-joining method: a new method for reconstructing phylogenetic trees. Mol. Biol. Evol. 4, 406–425. https://doi.org/10.1093/oxfordjournals.molbev.a040454.

Sakers, K., Eroglu, C., 2019. Control of neural development and function by glial neuroligins. Curr. Opin. Neurobiol. 57, 163–170. https://doi.org/10.1016/j.conb.2019.03.007.

Scholl, F.G., Scheiffele, P., 2003. Making connections: cholinesterase-domain proteins in the CNS. Trends Neurosci. 26, 618–624. https://doi.org/10.1016/j.tins.2003.09.004.

Schulte, J., Tepass, U., Auld, V.J., 2003. Gliotactin, a novel marker of tricellular junctions, is necessary for septate junction development in Drosophila. J. Cell Biol. 161, 991–1000. https://doi.org/10.1083/jcb.200303192.

Shillington, A., Lamy, M., Vawter-Lee, M., Erickson, C., Saal, H., Comoletti, D., Abell, K., 2020. Case report: is catatonia a clinical feature of the natural progression of NLGN2-related neurodevelopmental disorder? J. Autism Dev. Disord. https://doi.org/10.1007/s10803-020-04531-2.

Shipman, S.L., Nicoll, R.A., 2012. A subtype-specific function for the extracellular domain of neuroligin 1 in hippocampal LTP. Neuron 76, 309–316. https://doi.org/10.1016/j.neuron.2012.07.024.

Silman, I., Sussman, J.L., 2008. Acetylcholinesterase: how is structure related to function? Chem. Biol. Interact. 175, 3–10. https://doi.org/10.1016/j.cbi.2008.05.035.

Singh, S.K., Stogsdill, J.A., Pulimood, N.S., Dingsdale, H., Kim, Y.H., Pilaz, L.J., Kim, I.H., Manhaes, A.C., Rodrigues Jr., W.S., Pamukcu, A., Enustun, E., Ertuz, Z., Scheiffele, P., Soderling, S.H., Silver, D.L., Ji, R.R., Medina, A.E., Eroglu, C., 2016. Astrocytes assemble thalamocortical synapses by bridging NRX1α and NL1 via hevin. Cell 164, 183–196. https://doi.org/10.1016/j.cell.2015.11.034.

Song, J.-Y., Ichtchenko, K., Sudhof, T.C., Brose, N., 1999. Neuroligin 1 is a postsynaptic cell-adhesion molecule of excitatory synapses. Proc. Natl. Acad. Sci. U.S.A. 96, 1100–1105. https://doi.org/10.1073/pnas.96.3.1100.

Speicher, S., Garcia-Alonso, L., Carmena, A., Martin-Bermudo, M.D., de la Escalera, S., Jiménez, F., 1998. Neurotactin functions in concert with other identified CAMs in growth cone guidance in Drosophila. Neuron 20, 221–233. https://doi.org/10.1016/s0896-6273(00)80451-1.

Südhof, T.C., 2017. Synaptic neurexin complexes: a molecular code for the logic of neural circuits. Cell 171, 745–769. https://doi.org/10.1016/j.cell.2017.10.024.

Sun, M., Xing, G., Yuan, L., Gan, G., Knight, D., With, S.I., He, C., Han, J., Zeng, X., Fang, M., Boulianne, G.L., Xie, W., 2011. Neuroligin 2 is required for synapse development and function at the Drosophila neuromuscular junction. J. Neurosci. 31, 687–699. https://doi.org/10.1523/JNEUROSCI.3854-10.2011.

Sussman, J.L., Harel, M.i, Frolow, F., Oefner, C., Toker, A., Goldman, L., Silman, I., 1991. Atomic structure of acetyicholinesterase from Torpedo californica: a prototypic acetylcholine-binding protein. Science 253, 872–879. https://doi.org/10.1126/science.1678899.

Takács, V.T., Freund, T.F., Nyiri, G., 2013. Neuroligin 2 is expressed in synapses established by cholinergic cells in the mouse brain. PloS One 8, e72450. https://doi.org/10.1371/journal.pone.0072450.

Talebizadeh, Z., Lam, D.Y., Theodoro, M.F., Bittel, D.C., Lushington, G.H., Butler, M.G., 2006. Novel splice isoforms for NLGN3 and NLGN4 with possible implications in autism. J. Med. Genet. 43, e21. https://doi.org/10.1136/jmg.2005.036897.

Tan, K., Duquette, M., Liu, J., Zhang, R., Joachimiak, A., Wang, J., Lawler, J., 2006. The structures of the thrombospondin-1 N-terminal domain and its complex with a synthetic pentameric heparin. Structure 14, 33–42. https://doi.org/10.1016/j.str.2005.09.017.

Tanaka, H., Miyazaki, N., Matoba, K., Nogi, T., Iwasaki, K., Takagi, J., 2012. Higher-order architecture of cell adhesion mediated by polymorphic synaptic adhesion molecules neurexin and neuroligin. Cell Rep. 2, 101–110. https://doi.org/10.1016/j.celrep.2012.06.009.

Thoumine, O., Marchot, P., 2017. A triad of crystals sheds light on MDGA interference with neuroligation. Neuron 95, 729–732. https://doi.org/10.1016/j.neuron.2017.08.001.

Tsigelny, I., Shindyalov, I.N., Bourne, P.E., Südhof, T.C., Taylor, P., 2000. Common EF-hand motifs in cholinesterases and neuroligins suggest a role for Ca2+ binding in cell surface associations. Protein Sci. 9, 180–185. https://doi.org/10.1110/ps.9.1.180.

Ushkaryov, Y.A., Petrenko, A.G., Geppert, M., Südhof, T.C., 1992. Neurexins: synaptic cell surface proteins related to the alpha-latrotoxin receptor and laminin. Science 257, 50–56. https://doi.org/10.1126/science.1621094.

Varoqueaux, F., Jamain, S., Brose, N., 2004. Neuroligin 2 is exclusively localized to inhibitory synapses. Eur. J. Cell Biol. 83, 449–456. https://doi.org/10.1078/0171-9335-00410.

Venema, D.R., Zeev-Ben-Mordehai, T., Auld, V.J., 2004. Transient apical polarization of gliotactin and coracle is required for parallel alignment of wing hairs in Drosophila. Dev. Biol. 275, 301–314. https://doi.org/10.1016/j.ydbio.2004.07.040.

Weill, M., Lutfalla, G., Mogensen, K., Chandre, F., Berthomieu, A., Berticat, C., Pasteur, N., Philips, A., Fort, P., Raymond, M., 2004. Insecticide resistance in mosquito vectors. Nature 423, 136–137.

Wittek, A., Hollmann, M., Schleutker, R., Luschnig, S., 2020. The transmembrane proteins M6 and anakonda cooperate to initiate tricellular junction assembly in epithelia of Drosophila. Curr. Biol. 30, 4254–4262.e5. https://doi.org/10.1016/j.cub.2020.08.003.

Xu, J., Xiao, N., Xia, J., 2010. Thrombospondin 1 accelerates synaptogenesis in hippocampal neurons through neuroligin 1. Nat. Neurosci. 13, 22–24. https://doi.org/10.1038/nn.2459.

Xu, X., Xiong, Z., Zhang, L., Liu, Y., Lu, L., Peng, Y., Guo, H., Zhao, J., Xia, K., Hu, Z., 2014. Variations analysis of NLGN3 and NLGN4X gene in Chinese autism patients. Mol. Biol. Rep. 41, 4133–4140. https://doi.org/10.1007/s11033-014-3284-5.

Yan, J., Oliveira, G., Coutinho, A., Yang, C., Feng, J., Katz, C., Sram, J., Bockholt, A., Jones, I.R., Craddock, N., Cook, E.H., Vicente, A., Sommer, S.S., 2005. Analysis of the neuroligin 3 and 4 genes in autism and other neuropsychiatric patients. Mol. Psychiatr. 10, 329–332. https://doi.org/10.1038/sj.mp.4001629.

Zeev-Ben-Mordehai, T., Mylonas, E., Paz, A., Peleg, Y., Toker, L., Silman, I., Svergun, D.I., Sussman, J.L., 2009b. The quaternary structure of amalgam, a Drosophila neuronal adhesion protein, explains its dual adhesion properties. Biophys. J. 97, 2316–2326. https://doi.org/10.1016/j.bpj.2009.07.045.

Zeev-Ben-Mordehai, T., Paz, A., Peleg, Y., Toker, L., Wolf, S.G., Rydberg, E.H., Sussman, J.L., Silman, I., 2009a. Amalgam, an axon guidance Drosophila adhesion protein belonging to the immunoglobulin superfamily: over-expression, purification and biophysical characterization. Protein Expr. Purif. 63, 147–157. https://doi.org/10.1016/j.pep.2008.09.019.

Zhang, C., Milunsky, J.M., Newton, S., Ko, J., Zhao, G., Maher, T.A., Tager-Flusberg, H., Bolliger, M.F., Carter, A.S., Boucard, A.A., Powell, C.M., Sudhof, T.C., 2009. A neuroligin-4 missense mutation associated with autism impairs neuroligin-4 folding and endoplasmic reticulum export. J. Neurosci. 29, 10843–10854. https://doi.org/10.1523/JNEUROSCI.1248-09.2009.